

Review

A Review on Abrasive Wear of Aluminum Composites: Mechanisms and Influencing Factors

Nima Valizade  and Zoheir Farhat * 

Department of Mechanical Engineering, Dalhousie University, 1360 Barrington Street, Halifax, NS B3J 2X4, Canada; nima.valizade@dal.ca

* Correspondence: zoheir.farhat@dal.ca

Abstract: Aluminum matrix composites (AMCs) find extensive use across diverse industries such as automotive, aerospace, marine, and electronics, owing to their remarkable strength-to-weight ratio, corrosion resistance, and mechanical properties. However, their limited wear resistance poses a challenge for applications requiring high tribological performance. Abrasive wear emerges as the predominant form of wear encountered by AMCs in various industrial settings, prompting significant research efforts aimed at enhancing their wear resistance. Over the past decades, extensive research has investigated the influence of various reinforcements on the abrasive wear behavior of AMCs. This paper presents a comprehensive review of the impact of different variables on the wear and tribological response of aluminum composites. This review explores possible wear mechanisms across various tribosystems, providing examples drawn from the analysis of existing literature. Through detailed discussions on the effects of each variable, conclusions are drawn to offer insights into optimizing the wear performance of AMCs.

Keywords: aluminum; wear; tribology; composite; reinforcement; abrasion; wear mechanisms



Citation: Valizade, N.; Farhat, Z. A Review on Abrasive Wear of Aluminum Composites: Mechanisms and Influencing Factors. *J. Compos. Sci.* **2024**, *8*, 149. <https://doi.org/10.3390/jcs8040149>

Academic Editor: Francesco Tornabene

Received: 27 February 2024

Revised: 30 March 2024

Accepted: 12 April 2024

Published: 15 April 2024



Copyright: © 2024 by the authors. Licensee MDPI, Basel, Switzerland. This article is an open access article distributed under the terms and conditions of the Creative Commons Attribution (CC BY) license (<https://creativecommons.org/licenses/by/4.0/>).

1. Introduction to Abrasive Wear of Aluminum Composites

The automotive, aerospace, and mineral processing industries frequently rely on aluminum alloys for their ability to provide a blend of high-performance, lightweight, and resistance to environmental conditions. Aluminum matrix composites typically exhibit higher hardness and mechanical strength compared to pure aluminum alloys. Moreover, the utilization of AMCs has demonstrated the potential to significantly enhance tribological properties, particularly in resisting sliding, abrasive wear, and seizure [1,2]. However, AMCs often exhibit lower ductility and fracture toughness. The superior mechanical properties of AMCs stem from the effective transfer of load to the reinforcements, which possess greater hardness and strength. The establishment of adequate bonding between the matrix and reinforcements is pivotal for ensuring the desired properties in AMCs [3].

There are various methods for producing aluminum composites, such as stir casting [4,5], powder metallurgy [6,7], centrifugal casting [8,9], ultrasonication-assisted stir casting [3,10], and spray casting [11,12]. Stir casting and powder metallurgy are the most common techniques and have been extensively researched due to their versatility, ease of use, and commercial feasibility. However, selecting the most suitable process for producing AMCs can be challenging because the nature of the technique directly influences several critical factors such as the amount of porosity, distribution and bonding of reinforcements, mechanical response, corrosion properties, and tribological performance [13].

Abrasive wear is a form of mechanical wear that arises when a harder material comes into contact with a metal surface, undergoing repeated sliding or impact, resulting in material removal. It is the most prevalent type of wear and is often referred to as scratching due to the longitudinal grooves or scratches that develop on the softer surface. This wear phenomenon is frequently encountered in industrial environments where metal

components are exposed to abrasive particles such as sand, grit, or mineral ores. These abrasive particles function similarly to small cutting tools, inducing micro-fractures, cracks, and deformation on the metal surface, ultimately leading to material loss and a shortened lifespan for the component [14].

The resistance to abrasion should not be universally considered as an inherent material property, as it is influenced by multiple factors, including operating conditions and the properties of the counterpart [15]. The extent of abrasive wear depends on several variables, such as the characteristics of the abrasive material, the hardness and toughness of both the metal surface and its counterpart, reinforcement size, and content, and the speed and load of sliding. Materials with higher levels of hardness, strength, and toughness typically exhibit greater resistance to abrasive wear. Nonetheless, even these materials can be susceptible to severe wear, necessitating costly repairs or replacements. To mitigate abrasive wear, various strategies like coating, hardening, or utilizing wear-resistant alloys can be employed [14].

2. Wear Mechanisms

Before delving into the factors that influence abrasive wear in aluminum composites, it is beneficial to understand the wear mechanisms at play in these materials. Wear failures are complex, often involving multiple mechanisms concurrently. This underscores the importance of understanding the potential wear mechanisms to effectively mitigate wear in industrial settings. Abrasion, being the predominant form of wear in AMCs, does not represent a singular mechanism but rather denotes a common type of damage resulting from various physical actions on materials [16]. Understanding its diverse micromechanisms is crucial for predicting and mitigating material loss and failures in industrial applications. At the microscale, abrasion occurs through plowing, cutting, and cracking when two materials come into contact during the wear process. These micromechanisms for material removal or displacement can happen either through the asperities on the harder surface or through detached third-body particles from one of the surfaces.

Abrasive wear can be broadly classified into two modes: two-body and three-body abrasion. In two-body abrasion, the asperities on the surface of the harder material cause deformation on the adjacent surface. Conversely, three-body abrasion is induced by loose hard particles sliding between surfaces. Understanding three-body abrasion is crucial in comprehending the wear behavior of metal matrix composites because reinforcement particles may escape from the surface under specific conditions, leading to three-body abrasion and an increase in the wear rate [17]. Figure 1 schematically illustrates the two distinct modes of abrasive wear. In the following discussion about the micromechanisms of abrasion, we will explore how each of these modes can come into effect.

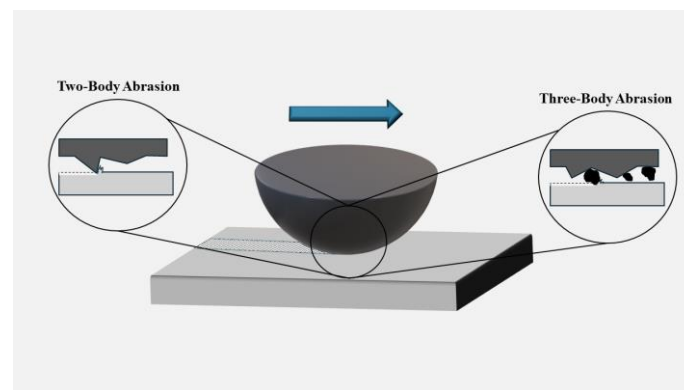


Figure 1. Schematic of two-body and three-body abrasion modes.

Several authors have demonstrated that AMCs exhibit superior wear resistance compared to aluminum matrices [18–21]. This is often attributed to the reinforcing agents'

increasing hardness, inversely affecting the wear rate according to Archard's law. It is worth noting that many researchers have suggested the benefits of reinforcing materials up to specific content, beyond which excessive addition may lead to severe wear [22–24]. In some cases, a brittle interface between the reinforcement and metallic matrix, such as Al_4C_3 phase in an Al/SiC composite system, can result in an unsatisfactory wear response [25]. Although there is relatively good agreement on the general trend of how reinforcement affects the wear rate of aluminum alloys, there is still no consensus on how wear mechanisms deviate when comparing AMCs to aluminum matrices. It is noteworthy to mention that there are classic models and theories that have been comprehensively reviewed and discussed in the literature. Thus, readers are encouraged to consult [26,27] to gain a deeper understanding of them. The major focus of the current review paper is on influencing factors on the abrasive wear of AMCs and micromechanisms involved in the abrasive wear of these materials. Table 1 summarizes the existing literature on the dominant wear mechanisms in aluminum matrix composites.

In the early 1980s, Hosking et al. [28] investigated the fabrication, mechanical, and wear characteristics of AMCs containing Al_2O_3 and SiC particles ranging in size from 1 to 142 μm . Various aluminum-copper wrought and cast alloys were used as the matrix materials. Testing against an AISI 52100 ball-bearing on a pin-on-disc machine revealed that composites with a high weight percentage of hard non-metals displayed impressive friction and wear properties. Their findings revealed that the unreinforced matrix alloys displayed adhesive wear mechanisms under the test conditions. Conversely, composites with a significant weight percentage of reinforcement demonstrated a pure abrasive wear mechanism on both the disc and the steel ball-bearing. This research shed light on the deviation in wear mechanisms observed in AMCs compared to the matrix alloy.

Solid lubricants like graphite, graphene, and carbon nanotubes (CNTs) exhibit remarkable anti-friction properties, making them ideal for self-lubricating composites [29–32]. Incorporating these carbon-based solid lubricant reinforcements into AMCs has been shown to induce significant shifts in wear mechanisms from adhesive to abrasive. For instance, as can be seen in Figure 2, Sharma et al. [33] demonstrated that the improved wear resistance of the Al-SiC-GNP (graphene nanoplatelets) hybrid composite, manufactured via friction stir processing (FSP), can be attributed to the layered structure of GNP, its extensive specific surface area, and the textured morphology of graphene flakes. While abrasion emerges as the primary wear mechanism in both the Al-SiC-Graphite and Al-SiC-GNP hybrid composites, delamination due to adhesion with the counter surface prevails in the Al-SiC-CNT hybrid composite.

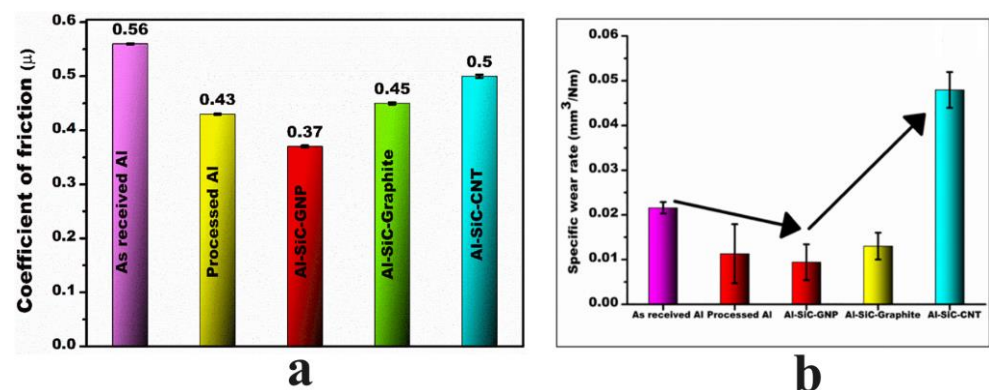


Figure 2. Comparison of (a) coefficient of friction (COF); (b) specific wear rate of AMCs consisting of various solid-lubricant reinforcements [33].

In general, the transition from adhesion to abrasion is anticipated when there is an increase in hardness, roughness, or the introduction of a second hard phase or solid-lubricant reinforcement on the surface. However, numerous factors play crucial roles, including the temperature at the contact surface, the impact of oxygen diffusion in tribofilms, the size

and composition of wear debris, the load-bearing capacity of the reinforcement, and the effective bonding between the reinforcement and matrix. These factors can significantly influence the overall wear behavior, leading to unexpected wear responses and mechanisms [29,34]. Therefore, it is essential to consider the complexity of the wear phenomenon when studying a tribosystem or conducting failure analysis, as a deep understanding of the wear mechanism is indispensable.

2.1. Microplowing

Microplowing is the most common micromechanism of abrasion, occurring predominantly in ductile materials. It is a consequence of the traversal of asperities (two-body) or abrasive particles (three-body) from a hard surface onto a softer one. Consequently, material displacement occurs sideways and in front of the asperities, creating ridges alongside abrasive grooves. Subsequently, the material loss transpires through the fracturing of these ridges due to the repetitive passage of the slider. Microplowing is considered a moderate wear mechanism compared to microcutting, which is known as a severe wear mechanism [35]. Scanning electron microscopy (SEM) image in Figure 3a illustrates how microplowing plastically deforms the surface and causes the formation of side edges. As depicted in Figures 3b and 5b, a lower coefficient of friction can be expected in microplowing compared to a wear process where microcutting is the dominant mechanism.

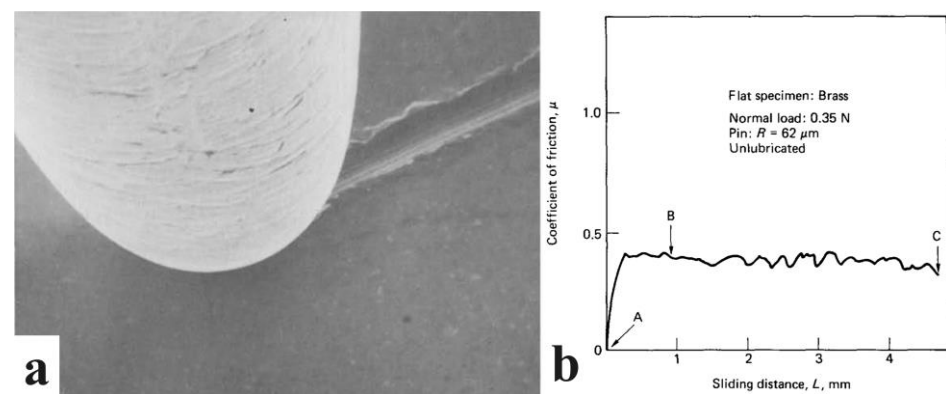


Figure 3. (a) SEM image of microplowing mechanism; (b) changes in coefficient of friction in sliding of a steel pin on brass for the plowing mode [36].

Pramanik [37] studied the wear resistance of AA6061/10 Vol.% Al_2O_3 produced by casting and hot extrusion. The wear resistance of the AMCs was found to be significantly higher than that of the corresponding matrix material. As shown in Figure 4a, unlike the non-linear wear behavior of the matrix material, the wear of the composite exhibits a linear pattern, making it easily predictable. While both materials share a similar wear mechanism, three-body abrasion was reported to be a distinctive feature in the case of AMCs. The higher material loss during wear for the aluminum matrix was found to be related to the detachment of debris from the surface due to adhesion and abrasion. On the other hand, in AMCs, the presence of reinforcement on the surface hinders detachment from the surface and limits the extensive three-body abrasion. The impact of reinforcement becomes apparent when comparing the worn surfaces of the AMCs and matrix in Figure 4b,c. On the AMC specimen, grooves appear scattered and dimpled, almost as if there are disruptions in the plowing line. In contrast, the grooves in the matrix material are evenly spaced and continuous. This observation implies that the presence of reinforcement particles restricts the extent of microplowing in AMCs.

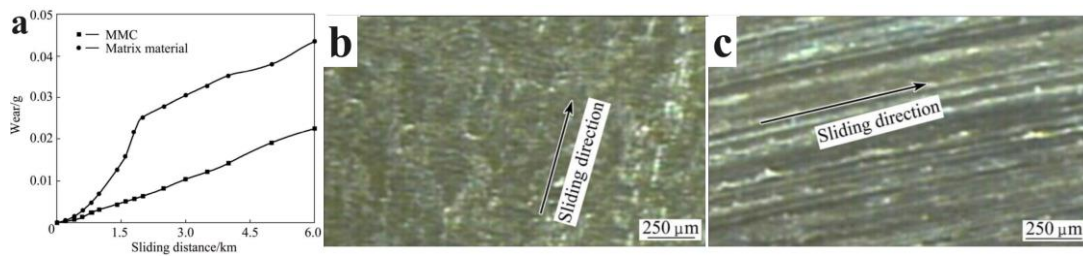


Figure 4. (a) Comparing wear performance of AA6061/Al₂O₃ 10 Vol.% with AA6061 matrix; (b) wear track of MMCs (c) wear track of matrix [37].

In another study, Jiang et al. [38] examined the wear characteristics of rheoformed AA2024 composites reinforced with Al₂O₃ nanoparticles. Their findings revealed an enhancement in the wear resistance of the composite compared to the matrix. Furthermore, an increase in the concentration of Al₂O₃ nanoparticles from 1 to 7 Vol.% was associated with a corresponding improvement in the wear resistance of the composite. However, a slight increase in the wear rate of MMCs was observed when the Al₂O₃ nanoparticle content reached 10%, attributed to reduced effective dispersion resulting from increased agglomeration. Their studies on the changes in wear mechanisms of MMCs indicated how the addition of Al₂O₃ nanoparticles can impede plastic deformation and microplowing in the MMCs, primarily due to the increased hardness of the composite.

2.2. Microcutting

The microcutting mechanism occurs in ductile materials and involves the cutting of material ahead of asperities (two-body) or abrasive particles (three-body), resulting in the formation of a chip. As depicted in Figure 5a, which illustrates the microcutting process, material removal occurs in the form of microchips ahead of the wear track. As shown in Figure 5b, the coefficient of friction is typically higher in microcutting mechanisms compared to microplowing (Figure 3b), leading to more severe wear [39].

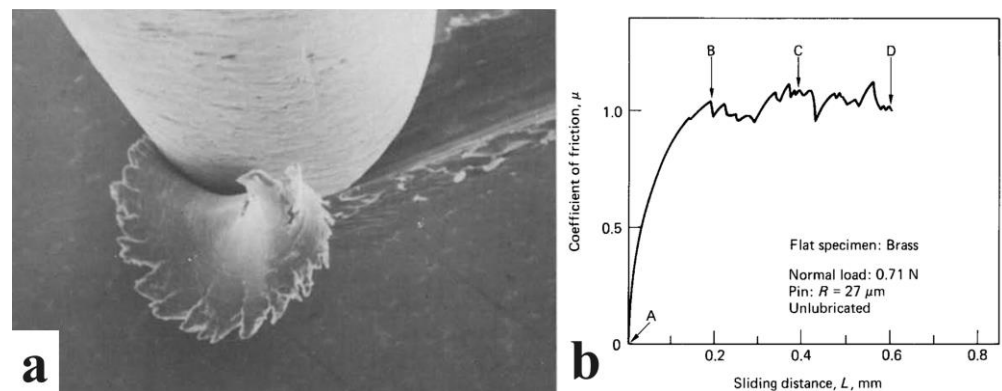


Figure 5. (a) SEM image of microcutting mechanism; (b) changes in coefficient of friction in sliding of a steel pin on brass for the cutting mode [36].

Wilson and Ball [40] conducted a study on the wear properties of AA6061/20 Vol.% SiC metal-matrix composite. They utilized both extruded and T6 heat-treated alloys, with and without SiC particles. Their research aimed to explore the shift in wear mechanism as contact stresses were reduced by varying the grit sizes of abrasive paper. Their results revealed a 6.3 times higher abrasion resistance in MMCs compared to unreinforced alloys. SEM studies of the wear track in MMCs showed a transition from microcutting to microplowing as contact stress decreased (or grit size increased). In contrast, no evidence of a similar transition in wear mode was observed for the unreinforced alloy, highlighting

the role of reinforcing particles in AMCs in impeding microcutting mechanisms during abrasive wear.

Contradictory findings regarding the impact of reinforcement on the microcutting mechanism in composites have also been documented. As previously discussed, the inclusion of harder reinforcement within the aluminum microstructure can elevate the overall hardness of the alloy, thereby enhancing its wear resistance. However, during the wear process of composite materials, the reinforcing particles may become dislodged from the composite, leading to three-body abrasion. The detached particles can cause the formation of microcuts and microcracks. Arendarchuck et al. [41] investigated the abrasive wear of A380/niobium carbide (NbC) composites using a dry sand/rubber wheel apparatus based on ASTM G65 standard [42]. While they observed deeper grooves and a higher wear rate for the matrix alloy, they noted shallow microcutting in the wear track of composites with various NbC content. The formation of these microcuts was attributed to the detachment of hard carbide particles. Similar findings were reported by Nieto et al. [43], where submicron size B₄C particles were found to reduce the wear resistance of the composite compared to the alloy. As can be seen in Figure 6, the detached particles caused microcutting on the surface and facilitated the material loss. The findings of such studies underscore the importance of considering the possibility of three-body abrasion when studying the wear mechanisms of AMCs.

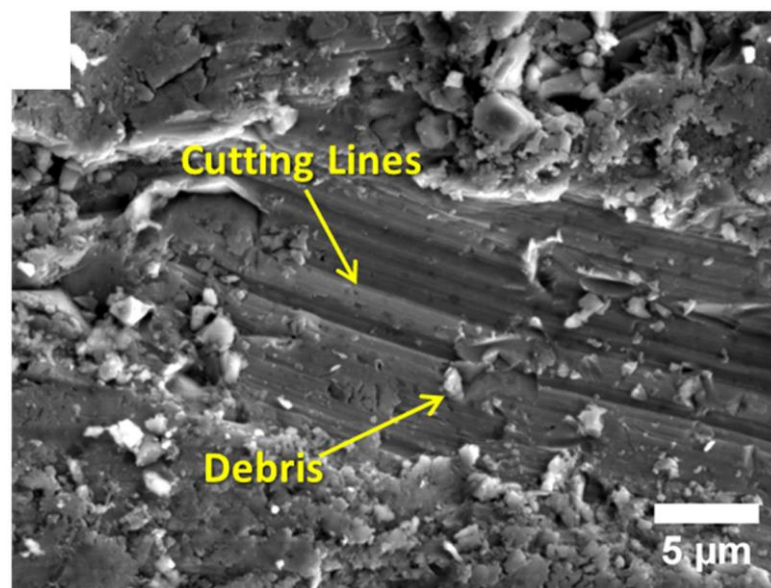


Figure 6. SEM image depicting cutting lines and debris within the scratch groove on the Al5083/5 Vol.% B₄C wear track [43].

2.3. Microcracking

The sliding of hard asperities over brittle materials can induce microcracking. Due to their inability to plastically deform, cracks form on the surface, leading to significant metal loss. The wear performance of composite materials relies heavily on the strength of the matrix/reinforcement interface. A strong interface that exceeds the minimum toughness of the constituent components typically leads to plowing as the primary wear mechanism, generating small wear debris compared to the size of the reinforcement. However, practical challenges such as chemical incompatibility, differences in thermal expansion coefficients, and the presence of impurities or voids can undermine this interface strength, potentially causing failure of the reinforcement either at the matrix/reinforcement interface or within the reinforcement itself. In situations with a weak interface, abrasive movement can trigger interfacial failure and separation, while a strong interface combined with a reinforcement prone to fracturing can result in failure within the reinforcement, especially in severe wear conditions [44].

Bai et al. [45] examined the sliding wear behavior of A356/15–20 Vol.% SiC composites. These AMCs exhibited superior wear resistance compared to the matrix alloy, attributed to reduced material flow at the surface, absence of microcracking, and the formation of iron-rich layers during sliding. In the A356 matrix alloy, material flow at the rubbing surface was prominent, with material curling along the walls and detaching, as depicted in Figure 7a. Additionally, subsurface microcracking, as shown in Figure 7b, significantly contributed to the alloy's high wear rate. The degree of material flow and debris formation is heightened with pressure. Incorporating SiC particles into the matrix proved advantageous in resisting material flow and subsurface cracking. As depicted in Figure 7c,d for AMCs, SiC particles engaged in the wear process by reducing microcracking and material flow.

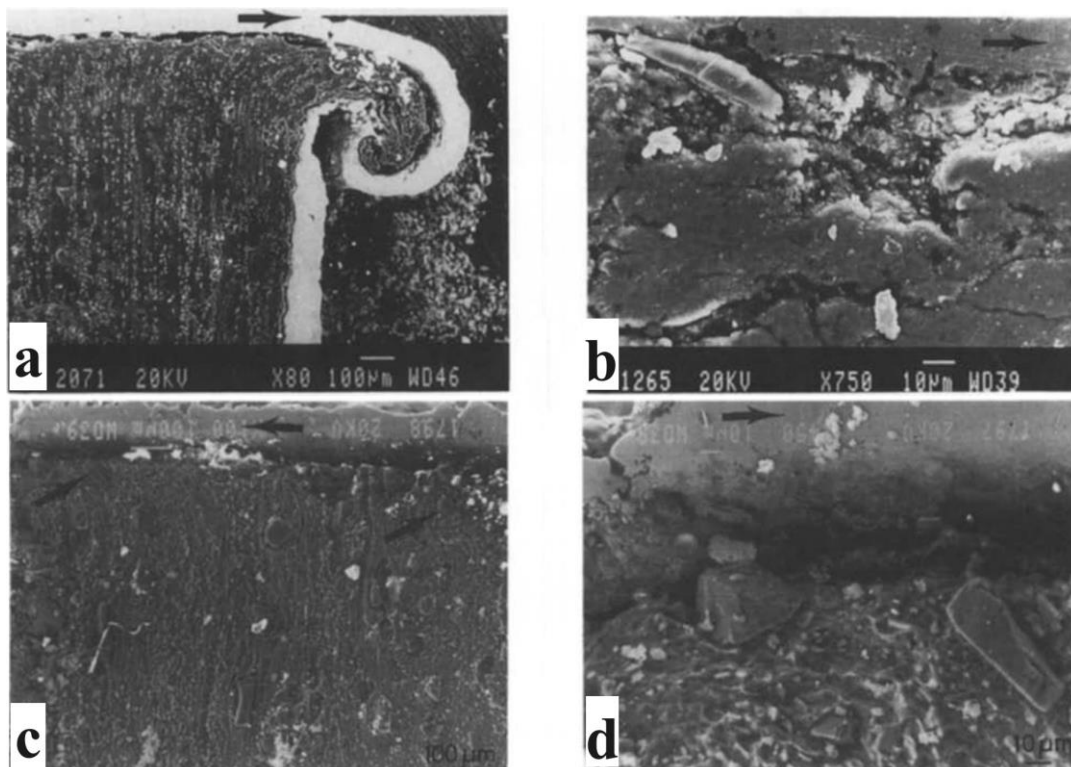


Figure 7. SEM micrographs depicting cross-sectional views of worn surfaces aligned parallel to the wear tracks and perpendicular to the worn surface (a) worn surface of A356 matrix alloy under 26 MPa load; (b) magnified section of (a) highlighting debris on the brink of detachment as a result of subsurface microcracking; (c) worn surface of 25 Vol.% SiC composite specimen at 26 MPa, featuring identifiable SiC particles; (d) magnified section of (c) (arrows indicate the sliding direction) [45].

Yan and Zhang's study [46] documented the occurrence of microcracks within the reinforcement phase of both Al/Al₂O₃ and Al/SiC composites, while no cracking was observed in the matrix alloys. These cracks were identified as fractures within the reinforcement material, forming behind the indenter during wear. As the indenter slid across the work material surface, horizontal compressive stress was generated in front of the indenter, accompanied by corresponding tensile stress behind it. Notably, distinctive features included fractured Al₂O₃ and SiC particles on the groove surface, suggesting that these ceramic particles were either fractured or dislodged by the passing indenter. Thus, in composites containing brittle reinforcements, particle fracture emerges as a significant factor in tribosystems, underscoring the importance of considering it during wear studies.

Table 1. Summary of wear mechanisms in aluminum matrix composites.

Alloy	Reinforcement	Counter Part	Reported Wear Mechanisms	Ref.
AA7075	0–8 Wt.% ZrO ₂	-	Adhesion and oxidation in alloy Abrasion and microcutting in composite	[18]
AA8011	0–8 Wt.% TiC	EN31 Steel	Abrasion and delamination in alloy Oxidation in composite	[19]
Pure Al	0–15 Wt.% B ₄ C	Al ₂ O ₃	Abrasion in alloy and composite Finer grooves in composites	[21]
AA7050	0–2 Wt.% BN	-	Delamination, abrasion, and adhesion in alloy and composite BN acts as a solid lubricant	[22]
Pure Al	2 Wt.% CNT 0–5 Wt.% Graphene	-	Adhesion and delamination in alloy matrix Abrasion in composite	[30]
Pure Al	0–0.75 Wt.% CNT 0–16 Wt.% Fly Ash	EN31 Steel	More microplowing reported in composite with high CNT and more microcutting in composite with high fly ash	[31]
AA6061	SiC Graphite GNP CNT	Steel	Abrasion in Al-SiC-Graphite and Al-SiC-GNP Adhesion and delamination in Al-SiC-CNT	[33]
AA6061	10 Vol.% Al ₂ O ₃	Steel	Abrasion, adhesion, and oxidation in both composite and alloy Three-body abrasion and higher oxidation in the composite	[37]
AA2024	0–10 Vol.% Al ₂ O ₃	5Cr15 Steel	Adhesion and delamination as the dominant wear mechanisms in all specimens Shallower microplowing by increasing the reinforcement content	[38]
A380	0–15 Wt.% NbC	Silica abrasive	Three-body abrasion and microcutting mechanisms reported for the sample with the highest reinforcement content Shallower microplowing by increasing the reinforcement content	[41]
A356	10–20 Vol.% SiC	AISI 52100 Steel	Microcracking under high applied load Severe wear only happens in unreinforced sample SiC suppresses the transition to severe wear	[47]
AA7075	0–6 Wt.% SiC	EN31 Steel	Abrasion and adhesion in all samples Three-body abrasion under high loads for composites Shallower microplowing by increasing the reinforcement content	[48]
AA2024	0–9 Wt.% SiC	EN31 Steel	Microplowing increases with an increase in applied load Delamination occurs more under high applied load	[49]
AA2024	0–30 Wt.% Al ₂ O ₃	SiC paper	Shallower microplowing by increasing the reinforcement content Microcutting and microplowing significantly reduced in composites with large size and higher content of reinforcements	[50]
AA6351	0–3 Wt.% Si ₃ N ₄	Steel	Adhesion and delamination in alloy matrix Abrasion in composite Shallower microplowing by increasing the reinforcement content	[51]
AA7075	0–8 Wt.% Si ₃ N ₄	EN31 Steel	Delamination in alloy matrix Abrasion in composite	[52]
AA6351	0–20 Wt.% AlN	Steel	Adhesion in alloy matrix Abrasion in composite Shallower microplowing by increasing the reinforcement content	[53]
AA7075	0–9 Wt.% TiB ₂	AISI 52100 Steel	Shallower microplowing by increasing the reinforcement content Presence of reinforcement reduced microcutting and plastic deformation in the matrix alloy	[54]
AA7075	0–20 Vol.% B ₄ C	OHNS Steel	Similar wear mechanisms in alloy matrix and composites Less plastic deformation, microplowing, and microcutting in the composites	[55]

Table 1. Cont.

Alloy	Reinforcement	Counter Part	Reported Wear Mechanisms	Ref.
Pure Al	0–4 Wt.% Ti ₃ AlC ₂	45 Steel	Adhesion in matrix alloy Abrasion in the composite Excessive Ti ₃ AlC ₂ content led to microcracking and severe fatigue delamination wear Shallower microplowing by increasing the reinforcement content Self-lubrication in the composites	[56]
Pure	Ti ₃ AlC ₂	Steel	At low sliding speeds, the dominant wear mechanism was abrasion, and at higher sliding speeds, adhesion and delamination take over	[57]
AA7075	Ti ₃ AlC ₂	AISI D3 steel	Adhesion in the matrix alloy Adhesion/abrasion in the composite	[58]
AA6061	10 Vol.% SiC 0–5 Vol.% Graphite	Steel	Adhesion in the matrix alloy In Al/SiC composites, by increasing the reinforcement size, the wear mechanism changed from adhesion and microcutting to abrasion and delamination Abrasion was dominant in the hybrid composites	[59]
AA5252	0–7 Wt.% SiC	AISI 52100 Steel	Abrasion and adhesion under low applied load Adhesion under high applied load	[60]
AA7075	5 Wt.% Al ₂ O ₃	AISI 52100 Steel	Abrasion in low load and sliding velocity Delamination under the high applied load and severe delamination under high load and high sliding velocity Microcracking increased with applied load	[61]
A319 A336 A390	15 Wt.% SiC	Cast iron	Transition from mild wear to severe wear by an increase in applied load and sliding velocity	[62]
AA2024	0–5 Wt.% ZrC	AISI 52100 Steel	Under low applied load and sliding velocity, abrasion is the dominant mechanism, and tribochemical and adhesion are the secondary mechanism Under high applied load and sliding velocity, tribochemical is the dominant mechanism, and abrasion and adhesion are the secondary mechanisms	[63]

3. Effect of Reinforcement Material and Content

The high wear resistance of AMCs is attributed to the presence of particles that shield the metal matrix from wear. Studies have demonstrated that increasing the particle content in aluminum alloy matrix composites reinforced with ceramic particles can significantly improve their wear resistance [64,65]. Consequently, this has been the driving force for research efforts aimed at incorporating various ceramic reinforcements into aluminum alloys, particularly in industries such as automotive, aerospace, and electrical. While much research has centered on the addition of ceramic reinforcements, recent studies have begun to explore the influence of advanced novel reinforcements such as MAX phases.

3.1. Ceramic Reinforcements

Silicon carbide (SiC) stands out as the most extensively researched ceramic reinforcement incorporated into AMCs. The SiC particles are believed to function as load-bearing components, and their abrasive actions against the counter surface result in material transfer from the counter surface to the contact surface [47]. Various studies have focused on the formation and properties of Al/SiC composites produced through the stir-casting process. Some research has shown that the inclusion of SiC reinforcements into the aluminum matrix composite results in increased hardness, tensile strength, and wear resistance [66]. Kumar et al. [48] investigated the impact of SiC on AA7075, revealing enhancements in density, hardness, and tensile strength with SiC addition. Similarly, Laksmipathy and

Kulendran [67] documented significant improvements in wear resistance with the incorporation of SiC particles into AA7075. Pramila Bai et al. [45], in their study using a pin-on-disc machine, observed an increase in wear resistance as the SiC particle content rose from 15 to 25 Wt.% in an Al-7Si alloy. Powder metallurgy is another technique employed for producing aluminum composites with SiC reinforcements. Singh and Singla [68] fabricated aluminum–silicon carbide particulate composites using the mechanical alloying process of powder metallurgy. They found that achieving a uniform distribution of silicon carbide within the matrix was possible. Furthermore, they noted that an increase in the amount of reinforcement led to increased hardness, accompanied by a linear decrease in the wear rate upon addition of silicon carbide.

While all the aforementioned research conducted by various authors was in agreement regarding the significant role of reinforcement in establishing a wear-resistant composite and the consistent increase in wear resistance with the addition of reinforcing particles, the study by Alpas and Embury [69] took a different perspective. They examined the sliding wear behavior of a commercial AA2024 alloy reinforced with 20 Wt.% SiC particles and found results that were not fully consistent with previous works. Despite the fact that the composite's hardness nearly doubled due to reinforcement, their findings showed only a minimal reduction in the wear rate compared to previous expectations. However, in another study by Alpas and Zhang [47] on A356 with 10–20 Vol.% SiC, utilizing a block-on-ring type apparatus, the composites strengthened with SiC particles exhibited superior wear resistance compared to the unreinforced Al-7Si alloy under low loads. Selvakumar et al. [70] investigated the effect of SiC addition up to 15 Wt.% to Al-4%Cu alloy produced via powder metallurgy. They found that as the amount of SiC particles increased, microhardness and compression strength also increased, while thermal conductivity decreased. AMCs with 7.5 Wt.% SiC showed the best wear behavior, beyond which un-bonding of SiC from the matrix caused an increase in wear rate. Reduction in wear rate by increasing SiC content up to 5 Wt.% is also reported in another study [71]. Dey et al. [49] studied the effect of SiC content on the tribological behavior of aluminum composites, reporting a reduction in wear loss with an increase in reinforcement content up to 9 Wt.%. Adhesive wear was observed for the alloy, while abrasive wear was the dominant mechanism for the composite. Additionally, more fine grooves were found on the worn surface as the SiC content increased, aligning with the continuous increase in hardness and ultimate tensile strength (UTS).

Good wettability and uniform distribution of alumina particles in aluminum melt have attracted significant attention to the properties of Al/Al₂O₃ composites [72]. A decrease in the wear rate of AA2024/Al₂O₃ composites was observed. This decrease was noted as the volume fraction of Al₂O₃ particles increased while maintaining a constant particle size. Additionally, the study found that the wear rate decreased as the particle size increased while maintaining a constant volume fraction. Daoud et al. [73] examined the impact of Al₂O₃ on the mechanical and wear characteristics of the AA7075 alloy. Their research revealed that hardness and wear resistance increased with the volume fraction of Al₂O₃ particles compared to the matrix alloy. In a study by Kok and Ozdin [50], the sliding wear behavior of aluminum/10–30 Wt.% Al₂O₃ was investigated. Their research demonstrated that the wear resistance of the composites was significantly higher than that of the aluminum alloy, and this wear resistance further increased with higher content of Al₂O₃ particles. It is noteworthy to mention that reduction in wear resistance of Al/Al₂O₃ composites, compared to the alloy matrix, has been reported in some studies where an excessive amount of reinforcement has been added to the composite [38,74]. This leads to agglomeration and the formation of porosities in the microstructure, underscoring the importance of achieving uniform distribution of reinforcements and homogeneity of the composite in tribological properties.

SiC and Al₂O₃ remain the predominant reinforcements in aluminum due to their ready availability as materials sourced from the abrasives industry. Nevertheless, both SiC and Al₂O₃ demonstrate instability within aluminum alloys. SiC undergoes a reaction

with aluminum, resulting in the formation of the brittle Al_4C_3 phase, while Al_2O_3 reacts with alloying Mg to produce MgO or MgAl_2O_4 [75]. There is currently a growing interest in materials that are inherently compatible, such as Si_3N_4 , which forms thin, stable boundary layers of AlN or SiAlON [76]. Possessing a desirable combination of physical and mechanical properties, such as high strength, hardness, Young's modulus, low density, and improved wear resistance, silicon nitride (Si_3N_4) is reported to be a very suitable type of material for use in AMCs [77,78].

Mohanavel et al. [51] used stir casting to manufacture aluminum composites with 0–3 Wt.% of Si_3N_4 . They found a continuous increase in UTS, yield strength, hardness, impact strength, and compressive strength with increasing Si_3N_4 content in the microstructure. SEM micrographs confirmed the even distribution of the reinforcement in the composite. Dry sliding wear tests were conducted on the samples according to ASTM G99-04 standard [79] specifications. The results showed a steady decrease in wear rate with increasing reinforcement content regardless of the applied load. As can be seen in Figure 8, they also reported abrasive wear for the composite and adhesion for the matrix alloy. In another study on AA2219/ Si_3N_4 composites with 3 Wt.%, 6 Wt.%, and 9 Wt.% of reinforcement, it was shown that the addition of 6 Wt.% of Si_3N_4 to the alloy exhibited optimum wear behavior at all applied loads and velocities [80]. Similar trends in wear rate results were also reported by Manjunatha et al. [78]. Improvements in the mechanical and tribological response of AA7075 by the addition of up to 8 Wt.% of Si_3N_4 during the stir casting route have been reported in another study by Haq and Anand [52]. They reported a 37% improvement in wear resistance under a low load of 10 N and 61% under a high load of 50 N. The results of their study also showed an increase in COF up to 4 Wt.% of reinforcement, beyond which COF reduced. The SEM images indicated delamination wear below 4 Wt.% and plowing beyond.

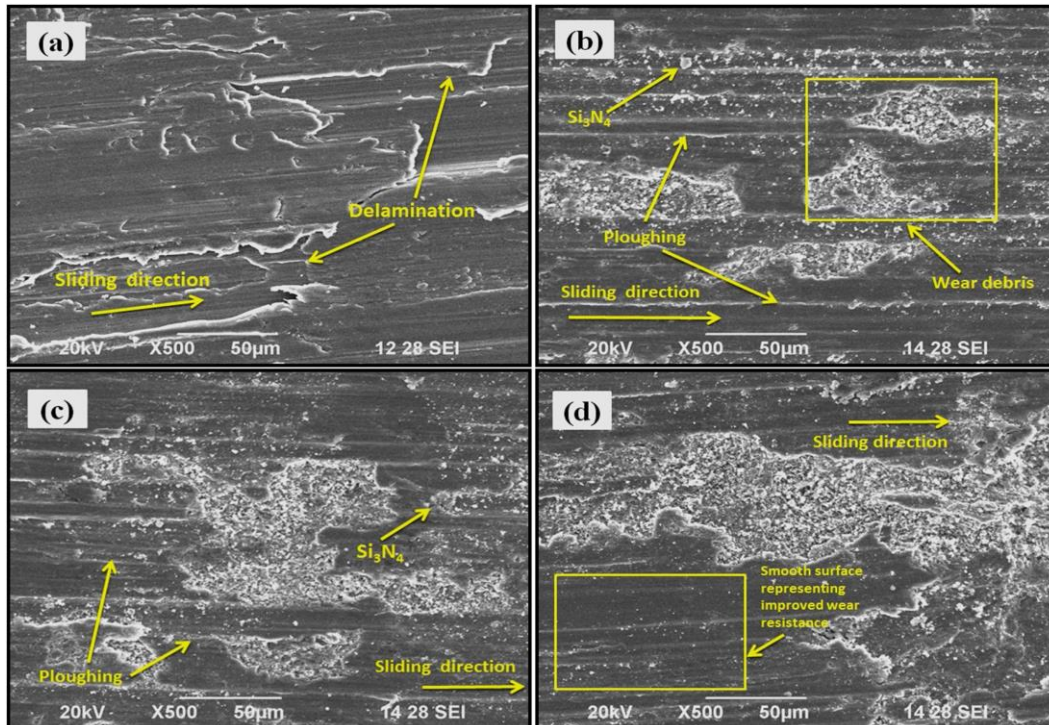


Figure 8. SEM images of the worn surface of AMCs with Si_3N_4 reinforcement under an applied load of 35N (a) 0 Wt.%; (b) 1 Wt.%; (c) 2 Wt.%; (d) 3 Wt.% of Si_3N_4 [51].

Aluminum nitride (AlN) possesses a desirable array of material characteristics, including strong thermal conductivity, low thermal expansion coefficient, relatively high electrical resistance, light weight, high Young's modulus, robust compressive strength and hardness,

excellent thermal stability, and resistance to corrosion and thermal shock. Additionally, it exhibits the capability to absorb high levels of energy. These inherent properties make AlN an attractive choice as a reinforcement material for lightweight aluminum-based metal matrix composites [81–83]. In terms of processing, AlN demonstrates superior wetting by molten aluminum compared to other common reinforcements like aluminum oxide (Al_2O_3). Moreover, AlN maintains a non-reactive nature with molten aluminum [84,85]. Fale et al. [86] studied the effect of adding Al/AlN to the aluminum metal matrix, reporting enhancement in the mechanical characteristics of the AMCs with an increase in the weight proportion of AlN particles. In another study by Mohanavel and Ravichandran [53], a composite of Al-Si-Mg (AA6351) with added AlN (4–20 Wt.%) filler was fabricated using an innovative and cost-effective melt stirring method. The results of the tests indicated that incorporating 20 Wt.% AlN into the Al composite resulted in enhanced wear resistance, hardness, yield strength, and tensile strength.

Although the aforementioned reinforcements constitute the most abundantly researched reinforcements in AMCs, other ceramics have also garnered attention based on their properties, which suit specific applications in specific industries. Titanium diboride (TiB_2)-based AMCs have recently been employed in the manufacturing of automobile pistons, vehicle drive shafts, and cylinder liners [87]. The impact of TiB_2 on AA7075 was examined by Rajan et al. [54], revealing that an increase in TiB_2 content resulted in improved wear resistance. According to research conducted by G. Singh et al. [88], the behavior of Al/ TiB_2 composites prepared by the in situ formation method was investigated. Their findings indicated that as the content of TiB_2 increased, the wear loss of the composites decreased. However, TiB_2 was found to have difficulty sustaining its effect with an increase in load and sliding distance. The study concluded that the improved tribological properties of aluminum matrix composites were primarily due to hard particles serving as reinforcement materials that can bear stress and reduce the formation of a mechanical mixing layer on the composite surface [89–91]. Kumar et al. [92] studied Al6061- TiB_2 composites produced via casting techniques, showing that increasing the amount of TiB_2 reinforcement resulted in higher values of hardness and UTS and lower volumetric wear loss. Furthermore, limited research work has been reported on AMCs reinforced with Boron Carbide particles (B_4C). The impact of B_4C on AA7075 was studied by Baradeswaran and Perumal [55], who found that the addition of particulates increased the hardness of the material, and the wear rate was significantly lower compared to the unmodified matrix material. Similarly, in their research on AA7075-TiC composites, Baskaran et al. [55] noted a reduction in wear rate as a result of adding TiC particles.

3.2. MAX Phases as Reinforcement

It is common knowledge that Al and Al alloys have poor tribological behavior; AMCs containing rigid ceramic particulates exhibit high specific strength and modulus, good wear resistance, and ease of machining [93,94]. These composites are becoming increasingly important for structural applications in aerospace, automotive, and other transport industries. However, the incorporation of hard ceramic particles in AMCs may pose a challenge for machining, necessitating the use of complex tools [95,96]. The $\text{M}_{n+1}\text{AX}_n$ phases, commonly known as MAX phases, constitute a group of over 60 thermodynamically stable nanolaminates with unique properties. They derive their name from their $\text{M}_{n+1}\text{AX}_n$ chemistry, wherein M represents an early transition metal, A signifies an A-group element, and X can be either C or N. MAX phases are hexagonal in shape and feature two formula units per cell. They boast remarkable characteristics such as high damage tolerance, resistance to thermal shock and creep, good lubrication, and machinability. Additionally, they are relatively soft, with Vickers hardness values ranging from 2 to 8 GPa. Some MAX phases also exhibit oxidation resistance. The incorporation of MAX phases into AMCs is predicted to enhance their mechanical properties and machinability. These attributes render MAX phases highly attractive for a wide range of structural applications [97–99].

Metal matrix composites reinforced with MAX phases recently hold significant importance both in theory and practical applications. Researchers have explored various types of MAXMET composites and their properties. For instance, Zhang et al. [100] discovered a new electro-friction composite material, $\text{Ti}_3\text{SiC}_2\text{-Cu}$. Gupta and colleagues developed composites using MAX phases and Ag that demonstrated solid lubrication over a broad temperature range [101,102]. Anasori et al. [103] reported the development of MAX phase composites with up to 80 Vol.% Mg, which are strong, stiff, lightweight, and easily machinable. These composites also exhibit high damping characteristics, with higher damping at lower stresses as the Mg volume fraction increases. Wang et al. [104] utilized a hot isostatic pressing technique to fabricate Al-matrix MAXMETs from pure Al and 40 Vol.% Ti_3AlC_2 powders. The yield strength of the Al/ Ti_3AlC_2 composite was found to be twice that of pure Al. Hu et al. [105] reported that an Al- Ti_2AlC alloy composite's specific strength was 50% higher than that of peak-aged Al alloy in an interpenetrating 40 Vol.% aluminum alloy composite. Recently, Kothalkar et al. [106] reported a high level of damping, up to 200 MPa greater than any metal-MAX phase composites reported in the literature, for Ti_3SiC_2 (MAX phase)—NiTi (Shape Memory Alloy). This discovery opens up the potential for multifunctional materials that incorporate MAX phases in metal matrix composites or ceramic matrix composites.

To expedite the rapid development and production of Al-MAX composites, innovative manufacturing techniques need to be explored. Wenyan et al. [56] utilized ultrasonic agitation casting to fabricate Al/ Ti_3AlC_2 composites and investigated their mechanical properties. Additionally, they studied the effect of various loads (10 N–40 N) and Ti_3AlC_2 content (1–4 Wt.%) on the tribological behavior of the composites. As anticipated, the addition of MAX phases successfully reduced the COF of the composites. While composite hardness increased with increasing reinforcement content, composites with 2 Wt.% of Ti_3AlC_2 were found to have the smallest grain size, highest UTS and yield strength, and lowest wear rate. As shown in Figure 9, adhesive wear was observed for the alloy and composites with 1 Wt.% reinforcement, while fatigue delamination occurred for the 3 Wt.% and 4 Wt.% composites in their study. Effective reduction in COF in Al/ $\text{Al}_3\text{Ti}/\text{Ti}_3\text{AlC}_2$ compared to Al alone was demonstrated in another study where friction stir processing was used to synthesize the composite in situ [57]. Another study on the in situ fabrication of AA7075/ Ti_3AlC_2 composites via friction stir processing confirmed a reduction in COF from nearly 1.1 to 0.3 as a result of the addition of MAX phases [58].

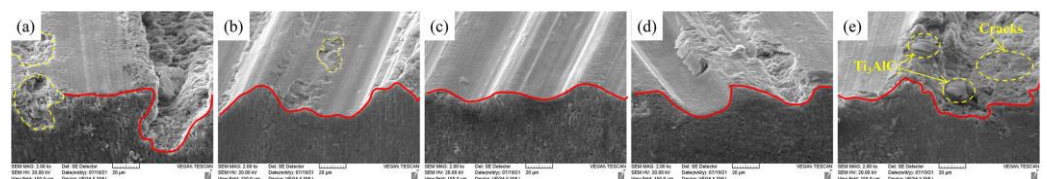


Figure 9. The worn surface of Al/ Ti_3AlC_2 composites with (a) 0 Wt.%; (b) 1 Wt.%; (c) 2 Wt.%; (d) 3 Wt.%; (e) 4 Wt.% reinforcement [56].

To summarize, it can be stated that the incorporation of reinforcement into aluminum composites can enhance hardness and mechanical properties, primarily by the Orowan strengthening effect and improving the load-bearing capability of the composite. Additionally, improved mechanical properties may arise from grain refinement and the Hall–Petch theory, wherein the reinforcement serves as nucleation sites during the solidification process [107]. However, the characteristics of the reinforcement–matrix interface play a critical role in determining the overall properties of the composite. Inadequate bonding between the matrix and reinforcement, formation of brittle phases, weak cohesion, or significant stress concentration at the interface can lead to deterioration of tribological properties. Furthermore, under high applied loads where the load exceeds the fracture toughness of the reinforcement, an increased wear rate may occur due to the occurrence of three-body abrasion conditions resulting from particle fracture or pull-out. This adverse effect can

counteract the beneficial influence of enhanced hardness on the overall wear characteristics of composites, thereby restricting the composite's overall tribological performance.

4. Effect of Reinforcement Size

It is widely recognized that the dimensions of reinforcement particles play a significant role in determining the properties of composites. However, the specific internal mechanism governing this relationship remains a topic of debate. It has been observed that due to residual thermal stress, there exists a maximum critical diameter for reinforcement particles. Beyond this threshold, there is a rapid decline in performance [108]. Skolianos and Kat-tamis [109] conducted research that showed that the specific wear rate of Al-4.5Cu-1.5Mg alloy composites reinforced with SiC particles increased as the size of the SiC particles increased from 10.7 to 29 μm , while the hardness decreased. In contrast, Mahdavi and Akhlaghi [59] and Liang et al. [110] have reported in their research that an increase in SiC reinforcement size results in an improvement in wear resistance. In another study, the effect of SiC reinforcement size on the wear resistance of AA5252 alloy, produced via powder compaction and extrusion, was investigated by Moazami-Goudarzi and Akhlaghi [60]. They used micro and nano SiC particles to fabricate the composite. The results showed that all composites regardless of their reinforcement size have higher hardness and wear resistance in comparison to the alloy matrix. But micro composite showed lower hardness and work of fracture in comparison to the nanocomposites. As can be seen in Figure 10, micro composites showed the lowest volume loss in the dry sliding wear test which was related to the good load-carrying ability of larger reinforcements. But under the critical transition load near 0.6 MPa, the volume loss increased sharply. The reason for such a sharp increase is attributed to the pulling out of large SiC micro particles from the matrix under higher loads. Removing the reinforcing particles led to the unprotected aluminum matrix coming into direct contact with the abrasive counterpart. They also studied the worn surface using EDS in order to analyze the mechanically mixed layer (MML) on the surface, which was expected to consist of Al and Fe and their oxides. The highest and lowest amount of Fe was found on the worn surface of micro composites under the load of 0.3 N and 0.9 N, respectively.

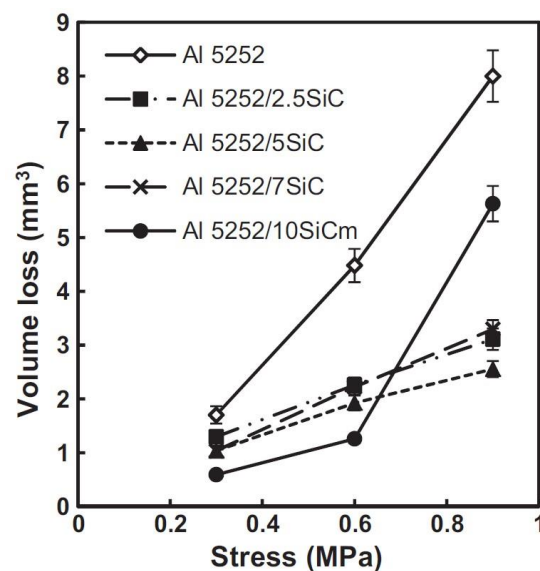


Figure 10. Effect of addition of nano and micro SiC reinforcement to wear behavior of AA5252 alloy and composites under various loads [60].

Rahman and Sirajudeen [111] fabricated AA7150/ Al_2O_3 composites via powder metallurgy using Al_2O_3 reinforcement with various sizes (21–165 nm). They reported an increase in microhardness with decreasing reinforcement size. Hosking et al. [28] were among the

pioneers who studied the effect of reinforcement size on the mechanical and tribological behavior of aluminum composites. In their work, AA2014 and AA2024 alloys were used to fabricate composites with Al_2O_3 reinforcement sizes ranging from 1 to 142 μm . They found that composites with larger particle sizes generally exhibited lower elongation, ductility, and also experienced lower weight loss in dry sliding wear tests. The same trend can be observed in other studies [61,112]. Aydin [61] investigated the effect of reinforcement size (0.3 μm , 2 μm , and 15 μm) on the wear performance of AA7075/ Al_2O_3 composites produced by powder metallurgy. They found that an increase in reinforcement size up to 15 μm led to higher hardness and wear resistance. As shown in Figure 11, larger particles effectively bear the load and shield the Al matrix. Conversely, smaller particles offer less protection due to their size being comparable to the surface roughness of the samples. No transition to severe wear was reported for composites with large reinforcement sizes. In this study, an interesting analysis of variance (ANOVA) was conducted to determine the contribution and effectiveness of various variables (load, sliding speed, and reinforcement size) on the final wear performance. It was reported that applied load had the highest contribution of 86.9% to the wear rate, while reinforcement size and sliding speed contributed 11.48% and 0.6%, respectively.

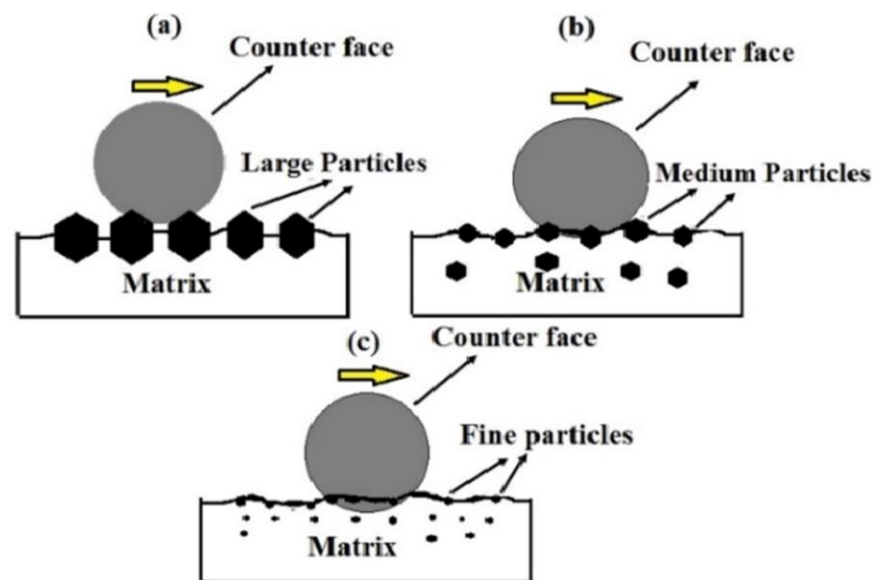


Figure 11. Schematic of the influence of reinforcement size on the tribology and wear behavior of aluminum composites: (a) large; (b) medium; (c) small reinforcement [61].

There are few studies available on the effect of TiO_2 reinforcement size on the wear behavior of aluminum composites. Arora et al. [113] fabricated LM13/ TiO_2 aluminum composites using fine (50–75 μm) and coarse (106–125 μm) rutile reinforcements via the stir-casting process. The study showed that composites with smaller reinforced particles exhibited roughly twice the wear resistance of composites with larger particles across a broad temperature range. Superior wear resistance for the composites with fine particles was suggested to result from higher hardness. A similar trend was found in other studies where TiO_2 reinforcements with two sizes of 20 μm and 40 μm were added to the composites. They reported higher tensile and impact strength, lower ductility, and wear rate for the composite with 20 μm titania [114].

In conclusion, reinforcement size can play a critical role in the overall performance of AMCs. Factors such as stress distribution and concentration, hardness, coefficient of thermal expansion, and inherent interface compatibility indicate that deviation in the size of reinforcement can alter the tribological properties of the composite [108]. Generally, it can be inferred that an increase in reinforcement size will enhance wear resistance up to a certain maximum size. However, the incorporation of particles with larger sizes

can significantly deteriorate the wear properties. It is noteworthy to mention that other parameters such as applied load must be taken into account as they will have a more pronounced effect on the final wear response. Table 2 summarizes the existing literature on the most influencing factors on abrasive wear of aluminum matrix composites.

Table 2. Summary of the influencing factors on abrasive wear of aluminum matrix composites.

Alloy	Reinforcement Material and Content	Reinforcement Size	Sliding Velocity	Applied Load	Observation/Remarks	Ref.
A356	0–25 Wt.% SiC	43 μm ave.	0.5 m/s	2–26 MPa	Wear resistance increases with increasing reinforcement content Significant plastic deformation and material flow in the sample without reinforcement, which increases with pressure	[45]
A356	10–20 Vol.% SiC	9–17 μm ave.	0.16–0.8 m/s	0.9–150 N	Wear rate increases with applied load and sliding velocity High levels of applied load lead to particle fracture and microcracking Presence of reinforcement suppresses the transition to severe wear, while severe wear occurs in unreinforced samples under high loads	[47]
Pure Al	0–20 Wt.% SiC	53–74 μm	300 rpm	10 N	Wear resistance increases with increasing reinforcement content	[66]
AA7075	0–6 Wt.% SiC	150 μm ave.	2.62 m/s	10–60 N	Wear resistance increases with increasing reinforcement content Wear rate increases with applied load and sliding velocity	[48]
AA1100	0–10 Wt.% SiC	40 nm ave.	1 m/s	20 N	Wear resistance increases with increasing reinforcement content	[71]
AA2024	0–9 Wt.% SiC	20 μm ave.	300 rpm	10–30 N	Wear resistance increases with increasing reinforcement content Wear rate increases with applied load	[49]
Al-4.5% Cu-1.5% Mg	0–0.29 Vol.% SiC	29 μm ave.	50–950 rpm	3.150 N	Wear resistance increases with increasing reinforcement content	[109]
Pure Al	15 Vol.% SiC	3.5 μm , 10 μm , and 20 μm ave.	0.01 m/s	2.2 MPa	Composites containing large reinforcements exhibit superior wear resistance Under wear conditions characterized by some impact component in the load, composites containing small particles are preferred	[110]
AA5252	0–7 Wt.% SiC	SiC nano: 60 nm ave. SiC micro: 63 μm ave.	0.5 m/s	0.3–0.9 MPa	Micro-composite showed the best wear resistance under 0.3 and 0.6 MPa applied load Nano-composite samples exhibited superior wear resistance under 0.9 MPa Abrasion and adhesion under 0.3 and 0.6 MPa applied load Adhesion under 0.9 MPa applied load	[60]
AA7075	0–20 Wt.% SiC	36 μm ave.	-	25–75	Wear resistance increases with increasing reinforcement content Wear rate increases with applied load	[115]

Table 2. Cont.

Alloy	Reinforcement Material and Content	Reinforcement Size	Sliding Velocity	Applied Load	Observation/Remarks	Ref.
A319 A336 A390	15 Wt.% SiC	32 μm ave.	0.4–1 m/s	30–150 N	The effect of applied load and sliding velocity on wear rate are dependent on each other Increase in load at low sliding velocity increases the wear rate gradually, while at high velocity with an increase in load, an abrupt increase in wear rate occurs Increase in sliding velocity under a low load leads to a decreased wear rate, while at high loads, the wear rate first decreases with an increase in sliding velocity, and above a certain velocity, an abrupt increase in wear rate occurs	[62]
AA6061	SiC Graphite GNP CNT	Graphite 44 μm ave. GNP 5–10 nm CNT 25 nm ave. dia. SiC 30 μm ave.	20 rpm	20 N	Al-SiC-GNP hybrid composite was reported to have the highest wear resistance due to self-lubrication and high thermal conductivity Al-SiC-CNT showed the highest wear rate	[33]
AA6061	10 Vol.% SiC 0–5 Vol.% Graphite	SiC: 19 μm , 93 μm , and 146 μm ave. Graphite: 75 μm ave.	0.5 m/s	20 N	Wear resistance increases with increasing reinforcement size Hybrid composites consistently showed higher wear resistance compared to Al/SiC composites.	[59]
AA7075 AA6061	0–20 Wt.% SiC 0–20 Wt.% Al_2O_3	36 μm ave.	-	25–75 N	Wear resistance increases with increasing reinforcement content in all composites Wear rate increases with applied load	[67]
AA6061	10 Vol.% Al_2O_3	6–18 μm	230–1480 rpm	0.14–1.1 MPa	Wear resistance is higher in composite Presence of reinforcements delayed the transition to sever wear Wear rate increases with applied load and sliding velocity for both samples, but in a more predictable way for the composite Increase in size of debris with increase in load and sliding velocity	[37]
AA2024	0–10 Vol.% Al_2O_3	60 nm ave.	0.8 m/s	30 N	Wear resistance is maximum in composite with 7 Vol.% reinforcement	[38]
AA7075	0–20 Vol.% Al_2O_3	60–80 μm	1 m/s	10–50 N	Wear resistance is maximum in composite with 10 Vol.% reinforcement Wear rate increases with applied load	[73]
AA2024	0–30 Wt.% Al_2O_3	16 μm and 32 μm	2 m/s	2 N and 5 N	Wear resistance increases with increasing reinforcement content and size The effect of reinforcement content was less than that of reinforcement size Wear rate increases with applied load	[50]
AA7150	5–25 Vol.% Al_2O_3	21 nm ave.	1 m/s	1–3 kg	Wear resistance increases with increasing reinforcement content Wear rate increases with applied load	[111]

Table 2. Cont.

Alloy	Reinforcement Material and Content	Reinforcement Size	Sliding Velocity	Applied Load	Observation/Remarks	Ref.
AA7075	5 Wt.% Al ₂ O ₃	0.3 μm, 2 μm, and 15 μm ave.	80–140 m/s	5–30 N	Wear resistance increases with increasing reinforcement size Wear rate increases with applied load Increase in applied load and sliding velocity changed the wear mechanism from abrasion to severe delamination and microcracking Wear resistance of the composites was mostly dependent on load, followed by particle size and sliding velocity	[61]
AA6061 AA2124 AA2014	0–20 Vol.% Al ₂ O ₃ 0–20 Vol.% Al ₂ O ₃	Al ₂ O ₃ : 14.1 μm and 19.1 μm ave. SiC: 15.8 μm and 2.4 μm ave.	0.2 m/s	0.9–350 N	Wear resistance increases with increasing reinforcement content and size Wear rate increases with applied load Above a certain applied load, reinforcement fracture causes three-body abrasion, and the wear rate of composite and alloy matrix become almost equal	[112]
AA2219	0–9 Wt.% Si ₃ N ₄	40 μm ave.	1.57–4.71 m/s	9.81–29.43 N	Wear resistance is maximum in composite with 6 Wt.% reinforcement Wear rate depends more on applied load and sliding velocity compared to reinforcement content Wear rate increases with applied load and sliding velocity	[78]
AA6351	0–3 Wt.% Si ₃ N ₄	30 nm ave.	1.5 m/s	35 N	Wear resistance increases with increasing reinforcement content	[51]
AA7075	0–8 Wt.% Si ₃ N ₄	40 μm ave.	1 m/s	10–50 N	Wear resistance increases with increasing reinforcement content Wear rate increases with applied load	[52]
AA7075	0–12 Wt.% Si ₃ N ₄	10–40 μm	3–5 m/s	1–3 kg	Wear resistance increases with increasing reinforcement content Wear rate was found to decrease with an increase in sliding velocity, whereas it increased with increasing sliding distance and load Sliding distance was the most dominating factor	[90]
Pure Al	0–5 Wt.% AlN	40–50 nm	2 m/s	10–30 N	Wear resistance increases with increasing reinforcement content Wear rate increases with applied load Wear resistance is more influenced by the applied load than by sliding distance	[86]
AA6351	0–20 Wt.% AlN	Less than 44 μm	1 m/s	10–30 N	Wear resistance increases with increasing reinforcement content	[53]
AA7075	0–9 Wt.% TiB ₂	Less than 2 μm	1.2 m/s	20 N	Wear resistance increases with increasing reinforcement content	[54]
AA6082	0–12 Wt.% TiB ₂	-	0.6–3.0 m/s	29.42–73.55 N	Sliding distance was the most dominating variable to influence the wear resistance followed by sliding speed, load, and reinforcement content	[88]

Table 2. Cont.

Alloy	Reinforcement Material and Content	Reinforcement Size	Sliding Velocity	Applied Load	Observation/Remarks	Ref.
AA6061	0–6 Wt.% TiB ₂	50 µm ave.	-	10–60 N	Wear resistance increases with increasing reinforcement content Wear rate increases with applied load	[92]
AA7075	0–20 Vol.% B ₄ C	16–20 µm	0.6 m/s	10–40 N	Wear resistance of composite was significantly higher than matrix alloy The wear rate slightly decreased with increasing reinforcement content Wear rate increases with applied load	[55]
Pure Al	0–15 Wt.% B ₄ C	14.17 µm ave.	0.07 m/s	5–10 N	Wear resistance increases with increasing reinforcement content Wear rate increases with applied load	[21]
AA5083	5 Vol.% B ₄ C	µB ₄ C: 1–7 µm ave. sµB ₄ C: 0.5 µm ave. nB ₄ C: 40 nm ave.	-	133 N	Maximum wear resistance is observed in the composite with nano reinforcement due to higher particle–matrix coherent interface Reinforcement pull-out and three-body abrasion become more significant factors in composites with larger reinforcements	[43]
AA8011	0–8 Wt.% TiC	10 µm ave.	1–5 m/s	10–30 N	Wear resistance is maximum in composite with 5 Wt.% reinforcement Wear rate increases with applied load	[19]
AA7075	0–8 Wt.% ZrO ₂	200 nm ave.	300 rpm	5 N	Wear resistance is maximum in composite with 4 Wt.% reinforcement	[18]
A380	0–15 Wt.% NbC	1.2 µm ave.	200 rpm	45 N	Wear resistance increases with increasing reinforcement content	[41]
LM13	20 Vol.% TiO ₂	50–75 µm 106–125 µm	1.6 m/s	49 N	Wear resistance increases with increasing reinforcement size	[113]
AA7075	0.1–0.5 Wt.% GNPs	5–30 nm	-	-	Wear resistance increases with increasing reinforcement content Wear resistance is improved in composites due to the self-lubricating effect	[29]
Pure Al	2 Wt.% CNT 1–5 Wt.% Graphene	CNT 10–20 nm dia. Graphene 5–10 nm	-	10–30 N	Wear resistance increases with increasing reinforcement content Sel-lubricating effect only reported in composite with high amount of reinforcement	[30]
Pure Al	0.25–0.75 Wt.% CNT 4–16 Wt.% Fly Ash	CNT 10–15 nm ave. dia. Fly Ash 9.29 µm ave.	100–300 rpm	10–30 N	Wear resistance is maximum in hybrid composite with 0.25 Wt.% CNT and 8 Wt.% fly ash compared to other mono-reinforced and hybrid-reinforced composites Excess amount of CNT results in particle agglomeration and excessive amount of fly ash causes formation of voids in the composite Wear rate increases with applied load and sliding velocity	[31]

Table 2. Cont.

Alloy	Reinforcement Material and Content	Reinforcement Size	Sliding Velocity	Applied Load	Observation/Remarks	Ref.
AA7075	0–20 Wt.% Graphite	-	0.6–1 m/s	10–30 N	Wear resistance is maximum in composite with 5 Wt.% reinforcement Self-lubrication properties reported in composites Wear rate increases with increasing applied load and decreases with increasing sliding speed	[32]
Pure Al	2 Vol.% GNP	GNP 6–8 nm ave.	100 rpm	1 N	Wear resistance reduces in composite due to agglomeration Composite had lower COF value compared to matrix alloy	[34]
Pure Al	0–4 Wt.% Ti ₃ AlC ₂	-	100 rpm	10–40 N	Wear resistance is maximum in composite with 2 Wt.% reinforcement Excessive Ti ₃ AlC ₂ content led to severe fatigue delamination wear Delamination was intensified and abrasive grooves were greatly reduced with the load increased	[56]
Pure	Ti ₃ AlC ₂	-	0.01–1 m/s	1.5 MPa	Wear resistance of the composite was higher than matrix alloy Wear resistance was initially reduced by increasing the sliding velocity up to 0.5 m/s and then increased afterward	[57]
AA7075	Ti ₃ AlC ₂	5 µm ave.	0.4 mm/min	10 N	Wear resistance of the composite was higher than matrix alloy. Presence of reinforcement increases the thermal stability and lowers the tendency for plastic flow	[58]

5. Effect of Applied Load and Sliding Velocity

The wear behavior of aluminum alloys can be categorized into two different wear mechanisms: oxidative or mild wear and metallic severe wear. The “point of seizure” marks a specific sliding speed and load at which severe wear begins. A comprehensive understanding of the effect of load and sliding speed on tribological behavior can aid in improving seizure resistance [28]. Prior to the point of seizure, it has been observed that an increase in applied load leads to a higher wear rate [115]. On the other hand, it has been reported that by the introduction of reinforcements such as Al₂O₃ and SiC, the transition from mild to severe wear can be delayed to a higher level of normal load [116,117]. Rajeev et al. [62] studied the effect of sliding speed and load on the transition to severe wear for aluminum composites in the presence of SiC reinforcements. They reported a transition load behavior only at high sliding speeds. As can be seen in Figures 12 and 13 for A319/15 Wt.% SiC, mild oxidative wear and severe wear were found for loads below 60 N and above 90 N, respectively. For samples tested with loads between 60 N and 90 N, oxidative wear and sub-surface delamination wear were found.

The increase in wear rate with an increase in applied load has been attributed to the elevation in temperature and alterations in the MML. In a study by Zhou et al. [63], a thorough investigation was conducted to explain how an increase in normal load affects the wear rate. As shown in Figure 14, their findings indicated that a higher load results in the formation of a thick MML layer due to the elevated surface temperature. However, this thick MML layer primarily consists of oxides and defects, resulting in the detachment of large debris during the wear test and an increase in metal loss. EDS analysis revealed that an increase in the applied load results in a higher amount of oxygen and iron on the surface, confirming the presence of a thicker MML. It has been noted that the AA2024/ZrC

composite experiences abrasive wear as its primary wear mechanism, along with tribochemical reactions and adhesive wear at low loads and sliding speeds (18 N and 0.52 m/s). However, as the load and sliding velocity increase, the wear mechanism of the composite shifts towards the dominance of tribochemical reactions, with secondary abrasive and adhesive wear.

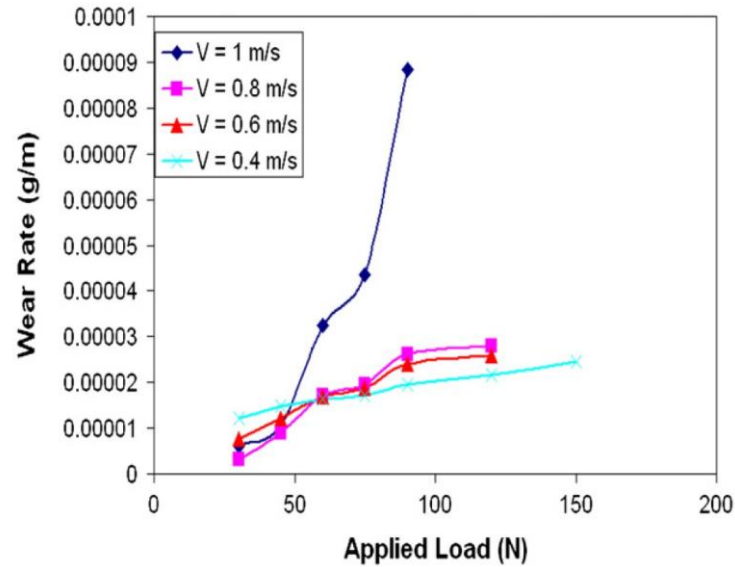


Figure 12. Wear rate against the normal load at various reciprocating velocities for A319/15 Wt.% SiC composite [62].

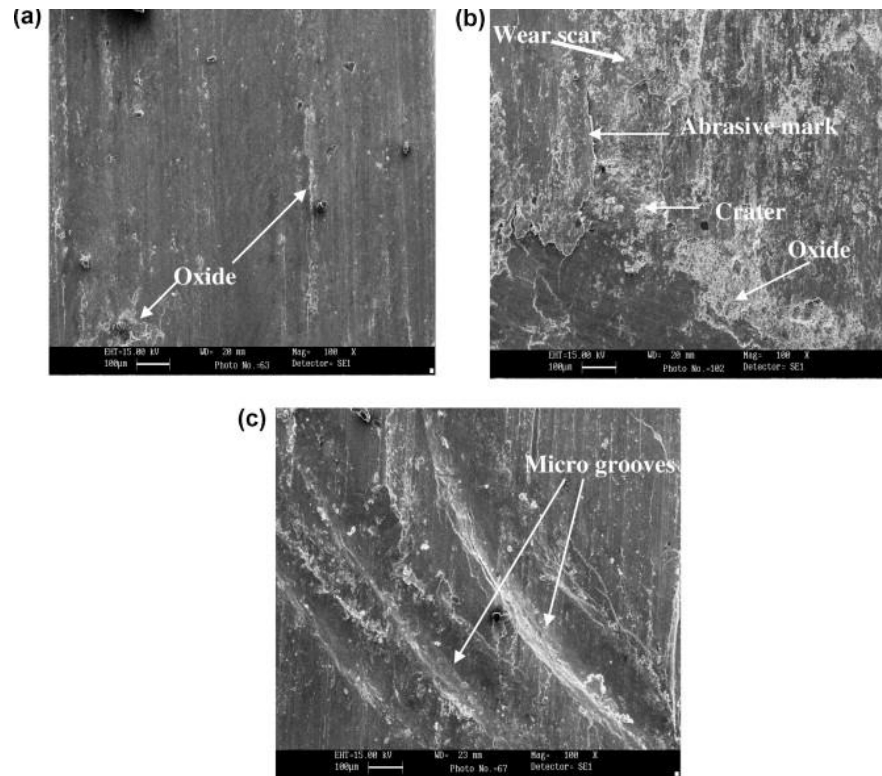


Figure 13. SEM images of A319/15 Wt.% SiC composite after dry sliding wear test under (a) load of 30 N and 0.4 m/s reciprocating velocity; (b) load of 60 N and 1 m/s reciprocating velocity; (c) load of 90 N and 1 m/s reciprocating velocity [62].

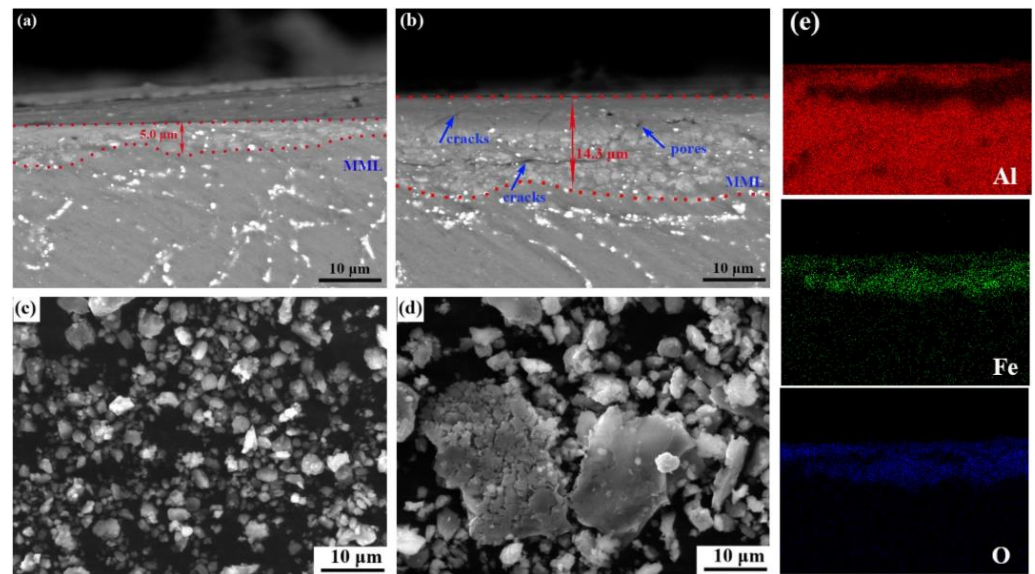


Figure 14. SEM image of cross section of AA2024/4Wt.% ZrC composite under the load of (a) 18N; (b) 54 N; (c) wear debris under 18 N; (d) 54 N. (e) EDS analysis of (b) [63].

6. Research Gaps for Future Studies

In the field of abrasive wear in aluminum matrix composites, several research gaps require further exploration. Firstly, while existing studies have investigated the influence of reinforcement size on AMCs properties, a deeper understanding is needed, especially concerning optimal particle sizes, particularly for less-studied reinforcements such as MAX phases. Despite the known benefits of using MAX phases in AMCs for improved wear properties, there remains a notable gap in understanding the specific mechanisms through which these reinforcements affect the tribological response of aluminum composites. Additionally, there is considerable opportunity for future research to leverage machine learning techniques to analyze the significance of various factors such as reinforcement content and size, and also applied load, and sliding speed on overall AMCs' tribological behavior. Lastly, investigating the formation and behavior of the mechanically mixed layer in AMCs is crucial for a comprehensive understanding of the wear mechanisms involved. Addressing these gaps will not only advance the fundamental knowledge but also pave the way for the development of more effective aluminum composites for diverse applications.

7. Conclusions

In this paper, a comprehensive review of the abrasive wear behavior of aluminum composites is provided, delving into the involved mechanisms and various influencing variables. These variables, including reinforcement content and size, applied load, and sliding velocity, have been thoroughly reviewed and investigated. The key outcomes are summarized below:

1. Reinforcement content significantly impacts the wear rate and tribological performance of AMCs. Generally, increasing reinforcement content enhances composite hardness and wear resistance. However, excessive reinforcement may lead to brittleness and inadequate bonding with the aluminum matrix. Achieving a homogeneous distribution of reinforcing particles is essential for optimal wear behavior.
2. Smaller reinforcements tend to be more effective in improving mechanical response and hardness, while larger reinforcements excel in load-bearing during wear conditions, offering better matrix protection.
3. Larger reinforcements are susceptible to being pulled out or broken under applied loads during wear.

4. At critical loads and sliding velocities, a transition from mild wear to severe wear can occur, leading to seizure. The presence of reinforcements can elevate the critical load and sliding velocity.
5. Elevated loads and sliding velocities increase surface temperature, promoting oxidation and potentially resulting in higher wear loss through the formation of defective mechanically mixed layers.

Author Contributions: Conceptualization, N.V. and Z.F.; writing—original draft preparation, N.V.; writing—review and editing, Z.F.; supervision, N.V. and Z.F.; project administration, N.V. and Z.F. All authors have read and agreed to the published version of the manuscript.

Funding: This work was funded by the Natural Sciences and Engineering Research Council of Canada (NSERC), grant # RGPIN-2023-03229.

Conflicts of Interest: The authors declare no conflicts of interest.

References

1. Ho, T.L.; Peterson, M.B. Wear formulation for aircraft brake material sliding against steel. *Wear* **1977**, *43*, 199–210. [[CrossRef](#)]
2. Prasad, S.V.; Rohatgi, P.K. Tribological Properties of Al Alloy Particle Composites. *JOM* **1987**, *39*, 22–26. [[CrossRef](#)]
3. Satish Kumar, T.; Nampootheri, J.; Shalini, S.; Thankachan, T. Microstructure and Wear Characteristics of Nano Y₂O₃ Particles Reinforced A356 Alloy Composites Synthesized through Novel Ultrasonic Assisted Stir Casting Technique. *Trans. Indian Inst. Met.* **2022**, *75*, 417–426. [[CrossRef](#)]
4. Pethuraj, M.; Uthayakumar, M.; Rajesh, S.; Abdul Majid, M.S.; Rajakarunakaran, S.; Niemczewska-Wójcik, M. Dry Sliding Wear Studies on Sillimanite and B4C Reinforced Aluminium Hybrid Composites Fabricated by Vacuum Assisted Stir Casting Process. *Materials* **2023**, *16*, 259. [[CrossRef](#)] [[PubMed](#)]
5. Kumar, D.; Singh, S.; Angra, S. Dry sliding wear and microstructural behavior of stir-cast Al6061-based composite reinforced with cerium oxide and graphene nanoplatelets. *Wear* **2023**, *516–517*, 204615. [[CrossRef](#)]
6. Surya, M.S.; Prasanthi, G. Effect of SiC Weight Percentage on Tribological Characteristics of Al7075/SiC Composites. *Silicon* **2022**, *14*, 1083–1092. [[CrossRef](#)]
7. Bai, Y.; Wei, J.; Lei, N.; Li, J.; Guo, Y.; Liu, M. Effect of VN and TiB₂-TiC_x Reinforcement on Wear Behavior of Al 7075-Based Composites. *Materials* **2021**, *14*, 3389. [[CrossRef](#)]
8. Sam, M.; Radhika, N. Influence of carbide ceramic reinforcements in improving tribological properties of A333 graded hybrid composites. *Def. Technol.* **2022**, *18*, 1107–1123. [[CrossRef](#)]
9. Kumar, K.; Dabade, B.M.; Wankhade, L.N.; Agrawal, E.; Chavhan, G. Experimental investigation on tribological performance and development of wear prediction equation of aluminium composite at elevated temperatures. *Int. J. Interact. Des. Manuf.* **2022**. [[CrossRef](#)]
10. Gupta, R.K.; Vashishtha, N.; Sapate, S.G.; Udhayabanu, V.; Peshwe, D.R. Influence of ultrasonic agitation on the abrasive wear characteristics of Al-Cu/2 vol% Grp composite. *Surf. Topogr. Metrol. Prop.* **2022**, *10*, 15001. [[CrossRef](#)]
11. Park, C.-S.; Kim, M.-H.; Lawley, A. Microstructure and wear response of spray cast Al-Si/SiCp composites. *Int. J. Powder Metall.* **1999**, *35*, 41–50.
12. Park, C.-S.; Kim, C.-H.; Kim, M.-H.; Lee, C. The effect of particle size and volume fraction of the reinforced phases on the linear thermal expansion in the Al-Si-SiCp system. *Mater. Chem. Phys.* **2004**, *88*, 46–52. [[CrossRef](#)]
13. Arunkumar, S.; Kumar, A.S. Studies on Egg Shell and SiC Reinforced Hybrid Metal Matrix Composite for Tribological Applications. *Silicon* **2022**, *14*, 1959–1967. [[CrossRef](#)]
14. Hutchings, I.; Shipway, P. 6—Wear by hard particles. In *Tribology*, 2nd ed.; Hutchings, I., Shipway, P., Eds.; Butterworth-Heinemann: Oxford, UK, 2017; pp. 165–236. [[CrossRef](#)]
15. Alpas, A.T.; Bhattacharya, S.; Hutchings, I.M. 4.5 Wear of Particulate Metal Matrix Composites. In *Comprehensive Composite Materials II*; Beaumont, P.W.R., Zweben, C.H., Eds.; Elsevier: Oxford, UK, 2018; pp. 137–172. [[CrossRef](#)]
16. Basu, B.; Kalin, M. Wear Mechanisms. In *Tribology of Ceramics and Composites*; John Wiley & Sons, Ltd.: Hoboken, NJ, USA, 2011; pp. 70–100. [[CrossRef](#)]
17. Singh, J.; Chauhan, A. Overview of wear performance of aluminium matrix composites reinforced with ceramic materials under the influence of controllable variables. *Ceram. Int.* **2016**, *42*, 56–81. [[CrossRef](#)]
18. Zhang, J.; Zhang, L.; Ma, H. Effect of ZrO₂ additions on the microstructure, mechanical and wear properties of ZrO₂/7075 aluminium alloy composite. *Mater. Today Commun.* **2023**, *37*, 107437. [[CrossRef](#)]
19. Golla, C.B.; Babar Pasha, M.; Rao, R.N.; Ismail, S.; Gupta, M. Influence of TiC Particles on Mechanical and Tribological Characteristics of Advanced Aluminium Matrix Composites Fabricated through Ultrasonic-Assisted Stir Casting. *Crystals* **2023**, *13*, 1360. [[CrossRef](#)]
20. Zhang, F.; He, Z.; Lu, K.; Zhan, Z.; Li, Z.; Wang, X. Interfacial microstructure and mechanical properties of 2124 aluminum alloy reinforced by AlCoCrFeNi high entropy alloy. *J. Mater. Res. Technol.* **2023**, *26*, 8846–8856. [[CrossRef](#)]

21. Bayrak, Y.; Kisasoz, A.; Sezer, R. Production and Characterization of B4C Content-Dependent Aluminum Matrix Composites Fabricated via Hot Pressing. *J. Mater. Eng. Perform.* **2023**. [[CrossRef](#)]
22. Thomas, S.; Menachery, N.; Thomas, L.P.; Santhosh, N.; Pradeep Kumar, G.S.; Hebbar, G.S. Influence of nano hexagonal boron nitride on the wear properties of aluminium alloy. *Adv. Mater. Process. Technol.* **2023**, 1–17. [[CrossRef](#)]
23. Alshalal, I.; Al-Zuhairi, H.M.I.; Abtan, A.A.; Rasheed, M.; Asmail, M.K. Characterization of wear and fatigue behavior of aluminum piston alloy using alumina nanoparticles. *J. Mech. Behav. Mater.* **2023**, *32*, 20220280. [[CrossRef](#)]
24. Hasan, S.A.; Zaki, M.U.; Hasan, F. Properties & characterization of reinforced aluminium metal matrix composites. *Mater. Today Proc.* **2023**. [[CrossRef](#)]
25. Bhansali, K.J.; Mehrabian, R. Abrasive Wear of Aluminum-Matrix Composites. *JOM* **1982**, *34*, 30–34. [[CrossRef](#)]
26. Bin Yusoff, Z.; Jamaludin, S.B.; Amin, D.M. Tribology and Wear Theory of Aluminium Composites: Review and Discussion. In Proceedings of the International Postgraduate Conference on Engineering (IPCE 2010), Perlis, Malaysia, 16–17 October 2010.
27. Deuis, R.L.; Subramanian, C.; Yellup, J.M. Dry sliding wear of aluminium composites—A review. *Compos. Sci. Technol.* **1997**, *57*, 415–435. [[CrossRef](#)]
28. Hosking, F.M.; Portillo, F.F.; Wunderlin, R.; Mehrabian, R. Composites of aluminium alloys: Fabrication and wear behaviour. *J. Mater. Sci.* **1982**, *17*, 477–498. [[CrossRef](#)]
29. Chak, V.; Chattopadhyay, H. Fabrication and heat treatment of graphene nanoplatelets reinforced aluminium nanocomposites. *Mater. Sci. Eng. A* **2020**, *791*, 139657. [[CrossRef](#)]
30. HR, M.N.; LH, M.; Malik, V.; GC, M.P.; Saxena, K.K.; Lakshmikanthan, A. Effect of microstructure, mechanical and wear on Al-CNTs/graphene hybrid MMC'S. *Adv. Mater. Process. Technol.* **2022**, *8*, 366–379. [[CrossRef](#)]
31. Devadiga, U.; Fernandes, P.; Buradi, A.; Emma, A.F. Significance of addition of carbon nanotubes and fly ash on the wear and frictional performance of aluminum metal matrix composites. *Eng. Rep.* **2024**, e12865. [[CrossRef](#)]
32. Baradeswaran, A.; Perumal, A.E. Wear and mechanical characteristics of Al 7075/graphite composites. *Compos. Part B Eng.* **2014**, *56*, 472–476. [[CrossRef](#)]
33. Sharma, A.; Narsimhachary, D.; Sharma, V.M.; Sahoo, B.; Paul, J. Surface modification of Al6061-SiC surface composite through impregnation of graphene, graphite & carbon nanotubes via FSP: A tribological study. *Surf. Coat. Technol.* **2019**, *368*, 175–191. [[CrossRef](#)]
34. Rengifo, S.; Zhang, C.; Harimkar, S.; Boesl, B.; Agarwal, A. Tribological Behavior of Spark Plasma Sintered Aluminum-Graphene Composites at Room and Elevated Temperatures. *Technologies* **2017**, *5*, 4. [[CrossRef](#)]
35. Coronado, J.J.; Sinatora, A. Effect of abrasive size on wear of metallic materials and its relationship with microchips morphology and wear micromechanisms: Part 1. *Wear* **2011**, *271*, 1794–1803. [[CrossRef](#)]
36. Hokkirigawa, K.; Kato, K. An experimental and theoretical investigation of ploughing, cutting and wedge formation during abrasive wear. *Tribol. Int.* **1988**, *21*, 51–57. [[CrossRef](#)]
37. Pramanik, A. Effects of reinforcement on wear resistance of aluminum matrix composites. *Trans. Nonferrous Met. Soc. China* **2016**, *26*, 348–358. [[CrossRef](#)]
38. Jiang, J.; Xiao, G.; Che, C.; Wang, Y. Microstructure, Mechanical Properties and Wear Behavior of the Rheoformed 2024 Aluminum Matrix Composite Component Reinforced by Al₂O₃ Nanoparticles. *Metals* **2018**, *8*, 460. [[CrossRef](#)]
39. Coronado, J.J. Effect of Abrasive Size on Wear. In *Abrasion Resistance of Materials*; Adamiak, M., Ed.; IntechOpen: Rijeka, Croatia, 2012. [[CrossRef](#)]
40. Wilson, S.; Ball, A. Wear resistance of an aluminium matrix composite. *Eng. Dev. Appl. Compos. Mater.* **1990**.
41. Arendarchuck, B.E.; Mayer, A.R.; Lourençato, L.A.; Lima, C.R.C.; Fals, H.D.C. Assessment of the Microstructure and Abrasive Wear Properties of an A380/NbC Aluminum Composite Produced by Stir Casting. *Int. J. Met.* **2023**. [[CrossRef](#)]
42. ASTM G65-15; Standard Test Method for Measuring Abrasion Using the Dry Sand/Rubber Wheel Apparatus. ASTM International: West Conshohocken, PA, USA, 2021. [[CrossRef](#)]
43. Nieto, A.; Yang, H.; Jiang, L.; Schoenung, J.M. Reinforcement size effects on the abrasive wear of boron carbide reinforced aluminum composites. *Wear* **2017**, 390–391, 228–235. [[CrossRef](#)]
44. Lee, G.Y.; Dharan, C.K.H.; Ritchie, R.O. A physically-based abrasive wear model for composite materials. *Wear* **2002**, *252*, 322–331. [[CrossRef](#)]
45. Bai, B.N.P.; Ramasesh, B.S.; Surappa, M.K. Dry sliding wear of A356-Al-SiCp composites. *Wear* **1992**, *157*, 295–304. [[CrossRef](#)]
46. Yan, C.; Zhang, L. Single-point scratching of 6061 Al alloy reinforced by different ceramic particles. *Appl. Compos. Mater.* **1994**, *1*, 431–447. [[CrossRef](#)]
47. Alpas, A.T.; Zhang, J. Effect of SiC particulate reinforcement on the dry sliding wear of aluminium-silicon alloys (A356). *Wear* **1992**, *155*, 83–104. [[CrossRef](#)]
48. Kumar, G.B.V.; Rao, C.S.P.; Selvaraj, N. Mechanical and dry sliding wear behavior of Al7075 alloy-reinforced with SiC particles. *J. Compos. Mater.* **2012**, *46*, 1201–1209. [[CrossRef](#)]
49. Dey, D.; Bhowmik, A.; Biswas, A. Effect of SiC Content on Mechanical and Tribological Properties of Al2024-SiC Composites. *Silicon* **2022**, *14*, 1–11. [[CrossRef](#)]
50. Kök, M.; Özdin, K. Wear resistance of aluminium alloy and its composites reinforced by Al₂O₃ particles. *J. Mater. Process. Technol.* **2007**, *183*, 301–309. [[CrossRef](#)]

51. Mohanavel, V.; Ashraff Ali, K.S.; Prasath, S.; Sathish, T.; Ravichandran, M. Microstructural and tribological characteristics of AA6351/Si₃N₄ composites manufactured by stir casting. *J. Mater. Res. Technol.* **2020**, *9*, 14662–14672. [[CrossRef](#)]
52. Ul Haq, M.I.; Anand, A. Dry Sliding Friction and Wear Behavior of AA7075-Si₃N₄ Composite. *Silicon* **2018**, *10*, 1819–1829. [[CrossRef](#)]
53. Mohanavel, V.; Ravichandran, M. Influence of AlN particles on microstructure, mechanical and tribological behaviour in AA6351 aluminum alloy. *Mater. Res. Express* **2019**, *6*, 106557. [[CrossRef](#)]
54. Michael Rajan, H.B.; Ramabalan, S.; Dinaharan, I.; Vijay, S.J. Effect of TiB₂ content and temperature on sliding wear behavior of AA7075/TiB₂ in situ aluminum cast composites. *Arch. Civ. Mech. Eng.* **2014**, *14*, 72–79. [[CrossRef](#)]
55. Baradeswaran, A.; Perumal, A.E. Influence of B₄C on the tribological and mechanical properties of Al 7075–B₄C composites. *Compos. Part B Eng.* **2013**, *54*, 146–152. [[CrossRef](#)]
56. Zhai, W.; Pu, B.; Sun, L.; Xu, L.; Wang, Y.; He, L.; Dong, H.; Gao, Y.; Han, M.; Xue, Y. Influence of Ti₃AlC₂ content and load on the tribological behaviors of Ti₃AlC₂p/Al composites. *Ceram. Int.* **2022**, *48*, 1745–1756. [[CrossRef](#)]
57. Madhu, H.C.; Edachery, V.; Lijesh, K.P.; Perugu, C.S.; Kailas, S. V Fabrication of Wear-Resistant Ti₃AlC₂/Al₃Ti Hybrid Aluminum Composites by Friction Stir Processing. *Metall. Mater. Trans. A* **2020**, *51*, 4086–4099. [[CrossRef](#)]
58. Ahmadiyad, S.; Momeni, A.; Bahmanzadeh, S.; Kazemi, S. Microstructure, tribological and mechanical properties of Al7075/Ti₃AlC₂ MAX-phase surface composite produced by friction stir processing. *Vacuum* **2018**, *155*, 134–141. [[CrossRef](#)]
59. Mahdavi, S.; Akhlaghi, F. Effect of the SiC particle size on the dry sliding wear behavior of SiC and SiC–Gr-reinforced Al6061 composites. *J. Mater. Sci.* **2011**, *46*, 7883–7894. [[CrossRef](#)]
60. Moazami-Goudarzi, M.; Akhlaghi, F. Wear behavior of Al 5252 alloy reinforced with micrometric and nanometric SiC particles. *Tribol. Int.* **2016**, *102*, 28–37. [[CrossRef](#)]
61. Aydin, F. The investigation of the effect of particle size on wear performance of AA7075/Al₂O₃ composites using statistical analysis and different machine learning methods. *Adv. Powder Technol.* **2021**, *32*, 445–463. [[CrossRef](#)]
62. Rajeev, V.R.; Dwivedi, D.K.; Jain, S.C. Effect of load and reciprocating velocity on the transition from mild to severe wear behavior of Al–Si–SiCp composites in reciprocating conditions. *Mater. Des.* **2010**, *31*, 4951–4959. [[CrossRef](#)]
63. Zhou, X.; Gao, Y.; Wang, Y.; Xiao, P.; Huang, X. Effects of ZrC particles, load and sliding speed on the wear behavior of the ZrC/2024Al composites. *Wear* **2022**, *506–507*, 204465. [[CrossRef](#)]
64. Sheasby, J.S.; Cohen, A.; Jia, C.D.; Sang, H.; Kenny, D. Wear of aluminium and Al-Si alloys in single-pass sliding against glass. *Wear* **1989**, *133*, 343–354. [[CrossRef](#)]
65. Kanth, V.K.; Pramila Bai, B.N.; Biswas, S.K. Wear mechanisms in a hypereutectic aluminium silicon alloy sliding against steel. *Scr. Metall. Mater.* **1990**, *24*, 267–271. [[CrossRef](#)]
66. Rahman, M.H.; Rashed, H.M.M. Al Characterization of Silicon Carbide Reinforced Aluminum Matrix Composites. *Procedia Eng.* **2014**, *90*, 103–109. [[CrossRef](#)]
67. Lakshmi pathy, J.; Kulendran, B. Reciprocating Wear Behaviour of 7075Al/SiC and 6061Al/Al₂O₃ Composites: A study of Effect of Reinforcement, Stroke and Load. *Tribol. Ind.* **2014**, *36*, 117–126.
68. Singh, R.; Singla, R. Tribological characterization of aluminium-silicon carbide composite prepared by mechanical alloying. *Int. J. Appl. Eng. Res.* **2012**, *7*, 1420–1423.
69. Alpas, A.T.; Embury, J.D. Sliding and abrasive wear behaviour of an aluminum (2014)-SiC particle reinforced composite. *Scr. Metall. Mater.* **1990**, *24*, 931–935. [[CrossRef](#)]
70. Selvakumar, V.; Muruganandam, S.; Senthilkumar, N. Evaluation of Mechanical and Tribological Behavior of Al–4%Cu–x%SiC Composites Prepared through Powder Metallurgy Technique. *Trans. Indian Inst. Met.* **2017**, *70*, 1305–1315. [[CrossRef](#)]
71. Alharbi, K.A.M.; Gamaoun, F.; Patra, I.; Kumar, T.C.A.; Gahar, A.K.; Sivaraman, R.; Galal, A.M. Mechanical properties and wear resistance of nano Al/SiC composites fabricated via APB. *Hum. Ecol. Risk Assess. Int. J.* **2023**, *29*, 463–470. [[CrossRef](#)]
72. Nourouzi, S.; Damavandi, E.; Rabiee, S.M. Microstructural and mechanical properties of Al–Al₂O₃ composites focus on experimental techniques. *Int. J. Microstruct. Mater. Prop.* **2016**, *11*, 383–398. [[CrossRef](#)]
73. Daoud, A.; El-Khair, M.; Abdel-Azim, A. Effect of Al₂O₃ Particles on the Microstructure and Sliding Wear of 7075 Al Alloy Manufactured by Squeeze Casting Method. *J. Mater. Eng. Perform.* **2004**, *13*, 135–143. [[CrossRef](#)]
74. Perumal Ezhilan, M.; Emmanuel, L.; Alagarsamy, S.; Meignanamoorthy, M. Investigations on microstructure, hardness and tribological behaviour of AA7075–Al₂O₃ composites synthesized via stir casting route. *Rev. Metal.* **2023**, *59*, e253. [[CrossRef](#)]
75. Dougherty, T.; Xu, Y. Properties and characterization of an aluminium–silicon nitride fibre powder metal composite. *SN Appl. Sci.* **2018**, *1*, 135. [[CrossRef](#)]
76. Saganuma, K. Strength and microstructure of silicon nitride/aluminum interface fabricated by squeeze cast brazing. *J. Eur. Ceram. Soc.* **1993**, *11*, 43–49. [[CrossRef](#)]
77. Maddaiah, K.C.; Kumar, G.B.V. Mechanical Characterization of AA357 Metal Matrix Composite with Reinforcement of Si₃N₄. *J. Test. Eval.* **2023**, *51*, 3255–3272. [[CrossRef](#)]
78. Manjunatha, C.J.; Narayana, V.; Raja, D.B.P. Investigating the Effect of Si₃N₄ Reinforcement on the Morphological and Mechanical Behavior of AA2219 Alloy. *Silicon* **2022**, *14*, 2655–2667. [[CrossRef](#)]
79. ASTM G99-17; Standard Test Method for Wear Testing with a Pin-on-Disk Apparatus. ASTM International: West Conshohocken, PA, USA, 2023. [[CrossRef](#)]

80. Manjunatha, C.J.; Prasad, C.D.; Hanumanthappa, H.; Kannan, A.R.; Mohan, D.G.; Shanmugam, B.K.; Venkatesgowda, C. Influence of Microstructural Characteristics on Wear and Corrosion Behaviour of Si_3N_4 -Reinforced Al2219 Composites. *Adv. Mater. Sci. Eng.* **2023**, *2023*, 1120569. [[CrossRef](#)]
81. He, X.; Ye, F.; Zhang, H.; Zhou, Z. Study on microstructure and thermal conductivity of Spark Plasma Sintering AlN ceramics. *Mater. Des.* **2010**, *31*, 4110–4115. [[CrossRef](#)]
82. Abe, H.; Sato, K.; Naito, M.; Nogi, K.; Hotta, T.; Tatami, J.; Komeya, K. Effects of granule compaction procedures on defect structure, fracture strength and thermal conductivity of AlN ceramics. *Powder Technol.* **2005**, *159*, 155–160. [[CrossRef](#)]
83. Liu, Z.; Wu, B.; Gu, M. Effect of hydrolysis of AlN particulates on corrosion behavior of Al/AlNp composite in neutral chloride solution. *Compos. Part A Appl. Sci. Manuf.* **2007**, *38*, 94–99. [[CrossRef](#)]
84. Zhang, Q.; Chen, G.; Wu, G.; Xiu, Z.; Luan, B. Property characteristics of a AlNp/Al composite fabricated by squeeze casting technology. *Mater. Lett.* **2003**, *57*, 1453–1458. [[CrossRef](#)]
85. Wang, J.; Yi, D.; Su, X.; Yin, F.; Li, H. Properties of submicron AlN particulate reinforced aluminum matrix composite. *Mater. Des.* **2009**, *30*, 78–81. [[CrossRef](#)]
86. Fale, S.; Likhite, A.; Bhatt, J. Compressive, tensile and wear behavior of ex situ Al/AlN metal matrix nanocomposites. *J. Compos. Mater.* **2015**, *49*, 1917–1928. [[CrossRef](#)]
87. Mohanavel, V.; Ravichandran, M.; Anandkrishnan, V.; Pramanik, A.; Meignanamoorthy, M.; Karthick, A.; Muhibbullah, M. Mechanical Properties of Titanium Diboride Particles Reinforced Aluminum Alloy Matrix Composites: A Comprehensive Review. *Adv. Mater. Sci. Eng.* **2021**, *2021*, 7602160. [[CrossRef](#)]
88. Singh, G.; Chan, S.L.-I.; Sharma, N. Parametric study on the dry sliding wear behaviour of AA6082-T6/TiB₂ in situ composites using response surface methodology. *J. Braz. Soc. Mech. Sci. Eng.* **2018**, *40*, 310. [[CrossRef](#)]
89. Idusuyi, N.; Olayinka, J.I. Dry sliding wear characteristics of aluminium metal matrix composites: A brief overview. *J. Mater. Res. Technol.* **2019**, *8*, 3338–3346. [[CrossRef](#)]
90. Mistry, J.M.; Gohil, P.P. Experimental investigations on wear and friction behaviour of Si_3N_4 p reinforced heat-treated aluminium matrix composites produced using electromagnetic stir casting process. *Compos. Part B Eng.* **2019**, *161*, 190–204. [[CrossRef](#)]
91. Nieto, M.D.; Abad, F.J.; Hernández-Camacho, A.; Garrido, L.E.; Barrada, J.R.; Aguado, D.; Olea, J. Calibrating a new item pool to adaptively assess the Big Five; [Nuevo banco de ítems para evaluar adaptativamente los cinco grandes]. *Psicothema* **2017**, *29*, 390–395. [[CrossRef](#)]
92. Kumar, G.B.V.; Gouda, P.S.S.; Chowdary, U.S.K.; Subash, T.; Vamsi, M.S.; Naresh, K. Development and experimental evaluation of titanium diboride particulate reinforcements on the Al6061 alloy composites properties. *Adv. Mater. Process. Technol.* **2022**, *8*, 1209–1225. [[CrossRef](#)]
93. Miracle, D.B. Metal matrix composites—From science to technological significance. *Compos. Sci. Technol.* **2005**, *65*, 2526–2540. [[CrossRef](#)]
94. Chen, Z.-C.; Takeda, T.; Ikeda, K. Microstructural evolution of reactive-sintered aluminum matrix composites. *Compos. Sci. Technol.* **2008**, *68*, 2245–2253. [[CrossRef](#)]
95. El-Gallab, M.; Sklad, M. Machining of Al/SiC particulate metal-matrix composites: Part I: Tool performance. *J. Mater. Process. Technol.* **1998**, *83*, 151–158. [[CrossRef](#)]
96. Ding, X.; Liew, W.Y.H.; Liu, X.D. Evaluation of machining performance of MMC with PCBN and PCD tools. *Wear* **2005**, *259*, 1225–1234. [[CrossRef](#)]
97. Zhang, Z.; Duan, X.; Jia, D.; Zhou, Y.; van der Zwaag, S. On the formation mechanisms and properties of MAX phases: A review. *J. Eur. Ceram. Soc.* **2021**, *41*, 3851–3878. [[CrossRef](#)]
98. Chirica, I.M.; Mirea, A.G.; Neațu, Ș.; Florea, M.; Barsoum, M.W.; Neațu, F. Applications of MAX phases and MXenes as catalysts. *J. Mater. Chem. A* **2021**, *9*, 19589–19612. [[CrossRef](#)]
99. Lei, X.; Lin, N. Structure and synthesis of MAX phase materials: A brief review. *Crit. Rev. Solid State Mater. Sci.* **2022**, *47*, 736–771. [[CrossRef](#)]
100. Zhang, Y.; Sun, Z.; Zhou, Y. Cu/Ti₃SiC₂ composite: A new electrofriction material. *Mater. Res. Innov.* **1999**, *3*, 80–84. [[CrossRef](#)]
101. Gupta, S.; Barsoum, M.W. On the tribology of the MAX phases and their composites during dry sliding: A review. *Wear* **2011**, *271*, 1878–1894. [[CrossRef](#)]
102. Gupta, S.; Filimonov, D.; Palanisamy, T.; El-Raghy, T.; Barsoum, M.W. Ta₂AlC and Cr₂AlC Ag-based composites—New solid lubricant materials for use over a wide temperature range against Ni-based superalloys and alumina. *Wear* **2007**, *262*, 1479–1489. [[CrossRef](#)]
103. Anasori, B.; Caspi, E.N.; Barsoum, M.W. Fabrication and mechanical properties of pressureless melt infiltrated magnesium alloy composites reinforced with TiC and Ti₂AlC particles. *Mater. Sci. Eng. A* **2014**, *618*, 511–522. [[CrossRef](#)]
104. Wang, W.J.; Gauthier-Brunet, V.; Bei, G.P.; Laplanche, G.; Bonneville, J.; Joulain, A.; Dubois, S. Powder metallurgy processing and compressive properties of Ti₃AlC₂/Al composites. *Mater. Sci. Eng. A* **2011**, *530*, 168–173. [[CrossRef](#)]
105. Hu, L.; Kothalkar, A.; O’Neil, M.; Karaman, I.; Radovic, M. Current-Activated, Pressure-Assisted Infiltration: A Novel, Versatile Route for Producing Interpenetrating Ceramic–Metal Composites. *Mater. Res. Lett.* **2014**, *2*, 124–130. [[CrossRef](#)]
106. Kothalkar, A.D.; Benitez, R.; Hu, L.; Radovic, M.; Karaman, I. Thermo-mechanical Response and Damping Behavior of Shape Memory Alloy–MAX Phase Composites. *Metall. Mater. Trans. A* **2014**, *45*, 2646–2658. [[CrossRef](#)]

107. Samal, P.; Vundavilli, P.R.; Meher, A.; Mahapatra, M.M. Influence of TiC on dry sliding wear and mechanical properties of in situ synthesized AA5052 metal matrix composites. *J. Compos. Mater.* **2019**, *53*, 4323–4336. [[CrossRef](#)]
108. Cai, Y.; Liu, Z.; Gong, K.; Zhang, Y. The effect of reinforcement particle size on the mechanical and fracture properties of glass matrix composites. *Heliyon* **2023**, *9*, e21895. [[CrossRef](#)] [[PubMed](#)]
109. Skolianos, S.; Kattamis, T.Z. Tribological properties of SiCp-reinforced Al-4.5% Cu-1.5% Mg alloy composites. *Mater. Sci. Eng. A* **1993**, *163*, 107–113. [[CrossRef](#)]
110. Liang, Y.N.; Ma, Z.Y.; Li, S.Z.; Li, S.; Bi, J. Effect of particle size on wear behaviour of SiC particulate-reinforced aluminum alloy composites. *J. Mater. Sci. Lett.* **1995**, *14*, 114–116. [[CrossRef](#)]
111. Rahman, M.A.; Sirajudeen, N. Influence of aging, varying particle size & volume fraction of Al₂O₃ particles on the hardness and wear behavior of Al 7150 alloy composite produced by hot uniaxial compaction method. *Mater. Res. Express* **2018**, *6*, 35006. [[CrossRef](#)]
112. Alpas, A.T.; Zhang, J. Effect of microstructure (particulate size and volume fraction) and counterface material on the sliding wear resistance of particulate-reinforced aluminum matrix composites. *Metall. Mater. Trans. A* **1994**, *25*, 969–983. [[CrossRef](#)]
113. Arora, R.; Kumar, S.; Singh, G.; Pandey, O.P. Influence of particle size and temperature on the wear properties of rutile-reinforced aluminium metal matrix composite. *J. Compos. Mater.* **2015**, *49*, 843–852. [[CrossRef](#)]
114. Srivallirani, K.; Rao, M.V. Assessing the role of reinforcement size and weight percentage on the mechanical and wear characteristics of Al7050-TiO₂-hBN hybrid composites. *Eng. Res. Express* **2023**, *5*, 15049. [[CrossRef](#)]
115. Lakshminpathy, J.; Kulendran, B. Effect of the amount of SiC, number of strokes, and applied load on the reciprocating wear behavior of Al-SiC composites. *Sci. Eng. Compos. Mater.* **2015**, *22*, 573–582. [[CrossRef](#)]
116. Pasaribu, H.R.; Sloetjes, J.W.; Schipper, D.J. The transition of mild to severe wear of ceramics. *Wear* **2004**, *256*, 585–591. [[CrossRef](#)]
117. Sharma, S.C.; Krishna, M.; Vizhian, P.S.; Shashishankar, A. Thermal effects on mild wear transition in dry sliding of aluminium 7075-short glass fibre composites. *Proc. Inst. Mech. Eng. Part D J. Automob. Eng.* **2002**, *216*, 975–982. [[CrossRef](#)]

Disclaimer/Publisher's Note: The statements, opinions and data contained in all publications are solely those of the individual author(s) and contributor(s) and not of MDPI and/or the editor(s). MDPI and/or the editor(s) disclaim responsibility for any injury to people or property resulting from any ideas, methods, instructions or products referred to in the content.